

Multi-Head Attention is a Multi-Player Game

Kushal Chakrabarti^{1,2} Nirmal Balachundar²

Abstract

Modern transformer attention is internally multi-agent — heads compete and coordinate — yet we train it as if it were a monolithic optimizer. We formalize this gap: cross-entropy training induces an implicit potential game among heads, and gradient descent converges to Nash equilibria with potentially unbounded inefficiency due to unpriced externalities (redundancy, correlated errors). Our main result bounds the Price of Anarchy by $\Gamma(G)$, the off-diagonal mass of a head interaction matrix capturing weight and gradient coupling. Under mild smoothness assumptions, we prove that both *excess hallucination probability* and *excess head redundancy* scale with PoA, unifying two distinct failure modes into a single mechanism. The bound is prescriptive: regularization that reduces $\Gamma(G)$ provably tightens PoA. We instantiate this as GAME-LoRA, combining Barlow Twins decorrelation with log-determinant coordination pressure. Experiments validate the theory: $\Gamma(G)$ predicts hallucination ($p < 0.05$), emergent coalitions exhibit selective coordination, and GAME-LoRA achieves up to 18% hallucination reduction (8% average) with no knowledge degradation — a Pareto improvement inaccessible to methods ignoring the game structure.

1. Introduction

Transformer attention heads are often described as learning specialized “circuits” that collaborate to solve tasks. But what governs this collaboration? Standard training optimizes a single loss (cross-entropy), treating the model as a monolithic function approximator. Yet internally, attention heads interact: they share the residual stream, compete for gradient signal, and influence each other’s representations. This gap—between multi-agent internals and single-agent training—has consequences.

¹Obviously Wrong, LLC, San Francisco, CA, USA ²South Park Commons, San Francisco, CA, USA. Correspondence to: Kushal Chakrabarti <kushalc@obviouslywrong.org>.

Preprint. February 3, 2026.

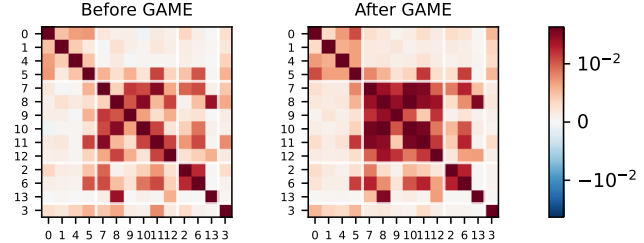


Figure 1. Attention heads form strategic coalitions when trained with game-aware regularization. We model multi-head attention as a multi-player game where heads compete for gradient credit while imposing unpriced externalities (redundancy, correlated errors) on each other. Standard cross-entropy training finds inefficient Nash equilibria; our method, GAME-LoRA, internalizes these externalities via Pigouvian taxes (log-determinant for compression, Barlow Twins for redundancy). The figure shows the head interaction matrix $G \in \mathbb{R}^{16 \times 16}$ for layer 19 of Qwen2.5-0.5B, reordered by spectral biclustering. **Left:** Before GAME-LoRA: heads show diffuse, unstructured coupling. **Right:** After GAME-LoRA: distinct coalitions emerge (white lines), with strengthened *intra*-coalition coordination and *inter*-coalition competition. This coalitional reorganization reduces the Price of Anarchy (Theorem 2.2), achieving best-in-class hallucination performance among five methods while preserving knowledge (Table 1).

We argue that standard training induces an *implicit game* among attention heads. Each head’s “strategy” is its learned representation; its “payoff” is its contribution to reducing task loss. Gradient descent finds Nash equilibria of this game. The problem: these equilibria have *unpriced externalities*. When head i duplicates head j , it wastes shared capacity (redundancy externality). When head i ’s errors correlate with head j ’s, ensemble variance grows (hallucination externality). Neither cost is reflected in the implicit payoff, so gradient descent finds equilibria with redundant heads, dead neurons, and elevated tail risk.

Our contribution is to make the game explicit:

- **A Game Theory of Attention.** We formalize multi-head attention as an implicit potential game (MultiHeadCE)—a game where individual gradients align with a shared objective—identify missing externality terms, and define an explicit externality-internalized game (MultiHeadPGAC).

- **Theoretical Foundations.** Under mild regularity assumptions, we derive Price of Anarchy bounds show-

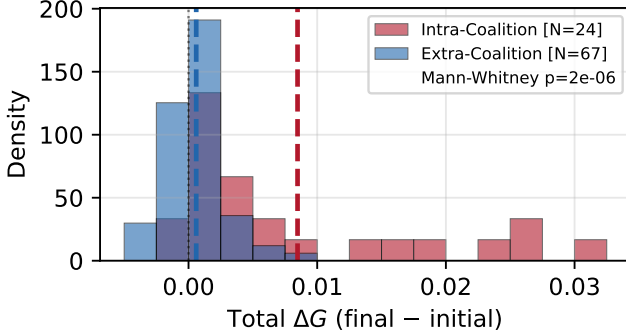


Figure 2. GAME-LoRA induces selective coordination, not uniform decorrelation. A naive interpretation of regularization losses would predict uniform weakening of all head interactions. Instead, we observe *strategic differentiation*: heads selectively strengthen coordination within emergent coalitions while reducing coupling across coalition boundaries. The histogram shows changes in pairwise coupling ΔG_{ij} (final – initial) for head pairs identified as intra-coalition (red, $N=24$) versus extra-coalition (blue, $N=67$) by spectral biclustering. Intra-coalition pairs strengthen significantly more (mean $\Delta G = 0.010$, dashed red) than extra-coalition pairs (mean $\Delta G \approx 0$, dashed blue), with $p = 2 \times 10^{-6}$ (Mann-Whitney). This selective reorganization mirrors coalition formation in cooperative game theory: heads that benefit from joint coordination form stable alliances, while heads serving distinct functions diversify—precisely the structure predicted by our externality-aware game formulation.

ing that hallucination probability and head redundancy are both controlled by the off-diagonal mass of the head interaction matrix (Theorem 2.2, Corollaries 2.1–2.2).

- **Practical Method.** GAME-LoRA instantiates MultiHeadPGAC in modern transformer models with lightweight LoRA adapters. It achieves best-in-class hallucination reduction (5/6 benchmark wins, 80% better than the runner-up) while preserving knowledge—not a tradeoff, but synergy.

2. A Game Theory of Attention

Why do transformers hallucinate? We propose that one source of hallucination is coordination failure among attention heads. Each head optimizes a shared loss, yet receives no signal about the costs it imposes on others—duplicating information already captured elsewhere, or making errors that compound with correlated errors from other heads. This is the classic structure of a game with externalities: individual rationality diverges from collective optimality.

We formalize this intuition by modeling each attention head as a strategic agent. Head i has parameters θ_i , produces output $h_i(x) \in \mathbb{R}^{d_h}$ (the attention-weighted value after the head-level computation but before the output projection W_O), and contributes to the shared residual stream via $W_O^{(i)} h_i(x)$. The key question: how do heads interact, and

when do those interactions lead to inefficiency?

2.1. Preliminaries

Notation. Let $X \sim \mathcal{D}$ denote inputs. The oracle truth is a probability vector $y_\star(x) \in \Delta^{d-1}$, inducing a label random variable $Y \mid X = x \sim y_\star(x)$. A model (with parameters w) induces a stochastic encoder $p_w(z_{1:H} \mid x)$ over H head streams Z_1, \dots, Z_H , and a decoder $q_w(y \mid z_{1:H})$.

Hallucination. Define the model prediction $\hat{y}_w(x) \in \Delta^{d-1}$ and the total-variation deviation

$$E_w(x) \triangleq \frac{1}{2} \|\hat{y}_w(x) - y_\star(x)\|_1, \quad (1)$$

$$H_\delta \triangleq \{x : E_w(x) \geq \delta\}. \quad (2)$$

The set H_δ captures inputs where the model’s prediction deviates substantially from ground truth—the “hallucination regime.” Our goal is to bound the probability mass on H_δ .

Redundancy. Define the conditional total correlation (multi-information) across streams

$$\text{TC}(Z_{1:H} \mid X) \triangleq \sum_{i=1}^H H(Z_i \mid X) - H(Z_{1:H} \mid X). \quad (3)$$

High TC means heads encode overlapping information given the input—a form of wasted capacity. When heads are conditionally independent given X , we have $\text{TC} = 0$; when they are perfectly correlated, TC is maximal.

Interaction matrix. We define a head interaction matrix that captures both *structural* coupling (through output projection weights) and *gradient* coupling (through backpropagated learning signal).

Definition 2.1 (Weight Coupling). For heads $i, j \in [H]$ with output projections $W_O^{(i)}, W_O^{(j)} \in \mathbb{R}^{d \times d_h}$, define

$$\omega_{ij} \triangleq \frac{\langle W_O^{(i)}, W_O^{(j)} \rangle_F}{\|W_O^{(i)}\|_F \|W_O^{(j)}\|_F}. \quad (4)$$

Definition 2.2 (Gradient Coupling). Let $\eta = \nabla_\ell \mathcal{L}_{\text{CE}}$ denote the gradient of cross-entropy loss with respect to logits. Define the backpropagated gradient through head i as $g_i = (W_O^{(i)})^\top \eta \in \mathbb{R}^{d_h}$, and

$$\rho_{ij} \triangleq \frac{\langle g_i, g_j \rangle}{\|g_i\| \|g_j\|}. \quad (5)$$

Definition 2.3 (Head Interaction Matrix). The head interaction matrix $G \in \mathbb{R}^{H \times H}$ has entries

$$G_{ij} \triangleq \omega_{ij} \cdot \rho_{ij}, \quad (6)$$

with interaction strength $\Gamma(G) \triangleq \|G - I\|_F$.

Table 1. Pricing externalities expands the Pareto frontier. Comparison on six hallucination benchmarks (HaluEval, MemoTrap, TruthfulQA) and five knowledge benchmarks (MMLU, NQ, PopQA, WikiText BPB, Winogrande). Baseline is LoRA with vanilla CE loss. Training-time baselines include DEACON, Disagreement, and ME (Maximizing Entropy); inference-time baselines include CAD and ActDec. *Key findings:* (1) GAME-LoRA achieves +8.1% hallucination improvement, 80% better than the next-best method (CAD, +4.5%), validating that Nash equilibrium selection via externality pricing yields superior solutions. (2) Unlike ActDec (−2.8% knowledge) and ME (−4.2% knowledge), GAME-LoRA preserves knowledge (−0.1%), confirming the Pareto improvement predicted by Corollary 2.3. Results averaged over 3 seeds; best in **bold**; WikiText is BPB (lower is better).

	Baseline	GAME-LoRA	CAD	Disagreement	ActDec	ME
<i>Hallucination</i>						
HE-Dial	0.458	0.491	0.479	0.471	0.458	0.455
HE-QA	0.376	0.445	0.417	0.391	0.376	0.395
HE-Summ	0.438	0.500	0.494	0.458	0.463	0.445
MemoTrap	0.642	0.650	0.641	0.641	0.642	0.642
TFQA-MC1	0.252	0.263	0.255	0.247	0.251	0.252
TFQA-MC2	0.401	0.412	0.392	0.399	0.416	0.419
<i>Knowledge</i>						
MMLU	0.477	0.469	0.479	0.472	0.476	0.471
NQ	0.066	0.067	0.066	0.063	0.067	0.057
PopQA	0.111	0.112	0.112	0.111	0.112	0.110
WikiText	0.784	0.786	0.779	0.777	0.923	0.825
Winogrande	0.573	0.565	0.569	0.580	0.575	0.573
<i>Overall</i>						
<i>Hallucination</i>	–	+8.0%	+4.5%	+1.5%	+1.5%	+1.8%
<i>Knowledge</i>	–	-0.1%	+0.4%	-0.6%	-2.8%	-4.2%

The product form $G_{ij} = \omega_{ij} \cdot \rho_{ij}$ captures the key insight that externalities arise only when heads are *both* structurally aligned (projecting to similar subspaces) *and* receiving correlated gradient signal. If either coupling vanishes, the pair contributes no inefficiency. We use G and $\Gamma(G)$ as tractable proxies for the intractable $\text{TC}(Z_{1:H} \mid X)$: under Gaussian assumptions, high off-diagonal mass in G implies high pairwise mutual information, which lower-bounds TC .

Definition 2.4 (Information Bottleneck Social Objective). Define the social objective via an information-bottleneck (IB) Lagrangian:

$$C_{\text{IB}}^*(w) \triangleq \underbrace{\mathbb{E}[-\log q_w(Y \mid Z_{1:H})]}_{\text{distortion}} \quad (7)$$

$$+ \beta_R \underbrace{\text{TC}(Z_{1:H} \mid X)}_{\text{redundancy}} \quad (8)$$

$$+ \beta_C \underbrace{\sum_{i=1}^H I(Z_i; X)}_{\text{compression}}. \quad (9)$$

All expectations are with respect to the joint distribution induced by $X \sim \mathcal{D}$, $Z_{1:H} \sim p_w(\cdot \mid X)$, and $Y \sim y_*(X)$.

This objective is derived directly from the multi-view Information Bottleneck (Tishby et al., 2000): each head should extract a minimal sufficient statistic of the input for predicting the target, while avoiding redundancy with other heads. A socially optimal configuration minimizes C_{IB}^* .

The question is whether decentralized gradient descent—where each head greedily minimizes its own loss—finds such configurations.

Definition 2.5 (Information Bottleneck Price of Anarchy). For a game \mathcal{G} with equilibrium set $\text{NE}(\mathcal{G})$, define

$$\text{PoA}(\mathcal{G}) \triangleq \frac{\max_{w \in \text{NE}(\mathcal{G})} C_{\text{IB}}^*(w)}{\min_w C_{\text{IB}}^*(w)}. \quad (10)$$

The Price of Anarchy measures how much worse the worst equilibrium is compared to the social optimum. A PoA of 1 means all equilibria are optimal; larger values indicate coordination failure. Our main results show that (i) standard cross-entropy training has potentially large PoA, and (ii) adding appropriate regularization reduces PoA, which in turn bounds hallucination probability.

2.2. MultiHeadCE: An Implicit, Incomplete Game

Standard transformer training minimizes cross-entropy loss via gradient descent. We show this implicitly defines a game among attention heads—but one where externalities go unpriced.

Definition 2.6 (MultiHeadCE). Partition parameters as $w = (\theta_1, \dots, \theta_H, \theta_{\text{rest}})$, where θ_i are head-specific parameters (player actions). Fix credit shares $\pi_i > 0$ —each head’s apportioned responsibility for the collective loss—with $\sum_{i=1}^H \pi_i = 1$. Define private costs (the loss each head

individually minimizes) for $i \in [H]$

$$C_i^{\text{CE}}(w) \triangleq \pi_i \mathbb{E}[-\log q_w(Y | Z_{1:H})] + \frac{\alpha}{2} \|\theta_i\|_2^2. \quad (11)$$

Theorem 2.1 (MultiHeadCE is a Weighted Potential Game).

Given [Definition 2.6](#), define the potential

$$\Phi_{\text{CE}}(w) \triangleq \mathbb{E}[-\log q_w(Y | Z_{1:H})] \quad (12)$$

$$+ \frac{\alpha}{2} \sum_{i=1}^H \frac{1}{\pi_i} \|\theta_i\|_2^2. \quad (13)$$

Then MultiHeadCE is a weighted potential game in the sense that, for each i ,

$$\nabla_{\theta_i} C_i^{\text{CE}}(w) = \pi_i \nabla_{\theta_i} \Phi_{\text{CE}}(w). \quad (14)$$

Consequently, any point w satisfying $\nabla_{\theta_i} C_i^{\text{CE}}(w) = 0$ for all i is a first-order (local) Nash equilibrium. Moreover, if Φ_{CE} has L_{Φ} -Lipschitz gradient, then gradient descent on Φ_{CE} with step size $\eta \in (0, 1/L_{\Phi})$ produces a sequence $\{w^t\}$ with $\min_{0 \leq t < T} \|\nabla \Phi_{\text{CE}}(w^t)\|_2^2 \rightarrow 0$ as $T \rightarrow \infty$.

Proof sketch. Differentiate C_i^{CE} and Φ_{CE} with respect to θ_i : both yield the same gradient direction (the shared CE term) plus a regularization term, with the π_i weighting ensuring $\nabla_{\theta_i} C_i = \pi_i \nabla_{\theta_i} \Phi$. Thus stationary points of Φ are Nash equilibria. Convergence follows from the standard descent lemma for smooth functions. \square

[Theorem 2.1](#) guarantees convergence to *some* Nash equilibrium, but says nothing about *which* one. The problem: MultiHeadCE has *unpriced externalities*. When head i duplicates head j , it wastes shared capacity (redundancy). When head i 's errors correlate with head j 's, ensemble variance grows and tail risk compounds (hallucination). Neither cost is reflected in C_i^{CE} , so gradient descent finds equilibria with redundant heads, dead neurons, and elevated hallucination.

2.3. MultiHeadPGAC: An Explicit Public-Goods + Anti-Coordination Game

To design the right incentives, we ask: what game are heads implicitly playing? The externalities above have recognizable structure: Redundancy arises when heads free-ride instead of differentiating; coverage gaps when none invests in minority features. These are the signature pathologies of *public-goods games* (under-provision) and *anti-coordination games* (failure to specialize). We posit CE training induces a PGAC game with missing incentives, and augment utilities with charges that restore them.

Definition 2.7 (MultiHeadPGAC). Define MultiHeadPGAC

by augmenting MultiHeadCE with IB-externality charges:

$$C_i^{\text{PGAC}}(w) \triangleq \pi_i \mathbb{E}[-\log q_w(Y | Z_{1:H})] \quad (15)$$

$$+ \frac{\alpha}{2} \|\theta_i\|_2^2 + \beta_C \tau_i^C(w) \quad (16)$$

$$+ \beta_R \tau_i^R(w), \quad (17)$$

where τ_i^C and τ_i^R approximate the marginal contribution of player i to $\sum_j I(Z_j; X)$ and $\text{TC}(Z_{1:H} | X)$ respectively.

We require two mild regularity conditions on the loss landscape and model parameterization.

Assumption 2.1 (Lipschitz Gradient). The cross-entropy loss \mathcal{L}_{CE} has L -Lipschitz gradient in the output projections $\theta = (W_O^{(1)}, \dots, W_O^{(H)})$:

$$\|\nabla_{\theta} \mathcal{L}_{\text{CE}}(\theta) - \nabla_{\theta} \mathcal{L}_{\text{CE}}(\theta')\| \leq L \|\theta - \theta'\|. \quad (18)$$

Assumption 2.2 (Bounded Projections). There exists $B > 0$ such that $\|W_O^{(i)}\|_F \leq B$ for all $i \in [H]$.

[Assumption 2.1](#) is standard for smooth optimization and holds for softmax cross-entropy with bounded logits. [Assumption 2.2](#) is trivially satisfied in practice via weight decay or explicit clipping, and implies bounded attention outputs $\|W_O^{(i)} a_i\| \leq B \|a_i\|$.

Theorem 2.2 (Multi-Head Games Have Price of Anarchy). Under [Assumptions 2.1–2.2](#), for any Nash equilibrium θ^{NE} with interaction matrix $G = G(\theta^{\text{NE}})$ satisfying $\Gamma(G)^2 < \alpha/L$:

$$\text{PoA(PGAC)} \triangleq \frac{C_{\text{IB}}^*(\theta^{\text{NE}})}{\min_{\theta} C_{\text{IB}}^*(\theta)} \leq \frac{1 + \beta_R + \beta_C}{1 - \frac{L}{\alpha} \Gamma(G)^2} \quad (19)$$

where $\Gamma(G)^2 = 2 \sum_{i < j} \omega_{ij}^2 \rho_{ij}^2$.

Proof sketch. The key insight is that $\Gamma(G)$ controls cross-head feedback: under [Assumptions 2.1–2.2](#), the off-diagonal Hessian blocks satisfy $\|\nabla_{\theta_i \theta_j}^2 D\| \leq L|G_{ij}|$, so head correlations amplify gradient perturbations along any path from equilibrium to optimum. This yields a smoothness inequality: the sum of costs under unilateral deviations to optimum is bounded by $(1 + \beta_R + \beta_C) C_{\text{IB}}^*(\theta^*)$ plus a feedback term $\frac{L}{\alpha} \Gamma(G)^2 C_{\text{IB}}^*(\theta^{\text{NE}})$. Nash optimality then implies equilibrium cost is at most this sum; rearranging under $\Gamma(G)^2 < \alpha/L$ isolates $C_{\text{IB}}^*(\theta^{\text{NE}})$ and produces the bound. Full proof in [subsection B.2](#). \square

[Theorem 2.2](#) is the theoretical engine of this paper: it converts a measurable property of head representations ($\Gamma(G)$, the off-diagonal mass of the interaction matrix) into a bound on equilibrium inefficiency. The bound is *prescriptive*: reducing $\Gamma(G)$ tightens PoA, providing theoretical motivation for decorrelation-based regularization. High $\Gamma(G)$ signals coordination failure: correlated heads free-ride on each other's signal (redundancy, [Corollary 2.2](#)) and amplify each other's errors into the tail (hallucination, [Corollary 2.1](#)).

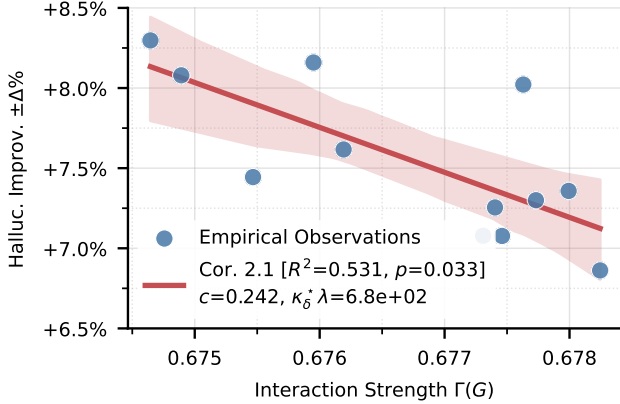


Figure 3. Instantiation of Corollary 2.1. Since excess hallucination $\propto \text{PoA} \propto 1/(1 - c \cdot \Gamma)$, we fit $\Delta H = a - \lambda/(1 - c \cdot \Gamma)$ to training trajectories. The fit achieves $R^2 = 0.53$ ($p < 0.05$) with bootstrap 95% prediction bands (shaded). **Non-vacuousness:** The fitted $c \cdot \Gamma \approx 0.2 \ll 1$ confirms the bound is finite and tight—reducing Γ yields proportional hallucination reduction.

Subspace optimization. Our bounds depend on $\Gamma(G)$, a function of activations, not parameters, and thus apply equally to full gradient descent and subspace methods like LoRA. Moreover, restricting strategy spaces can only reduce PoA: the worst-case equilibrium in a constrained game cannot exceed that in the full game.

Corollary 2.1 (Excess Hallucination Is Price of Anarchy). *Let $w^* \in \arg \min_w C_{\text{IB}}^*(w)$ denote the social optimum and assume $\Pr(H_\delta \mid w^*) > 0$. Define the constant $\kappa_\delta^* \triangleq C_{\text{IB}}^*(w^*)/(2\delta^2 \Pr(H_\delta \mid w^*))$, which depends only on w^* . Then, for any equilibrium $w^{\text{NE}} \in \text{NE}(\mathcal{G})$ of $\mathcal{G} \in \{\text{CE}, \text{PGAC}\}$,*

$$\frac{\Pr(H_\delta \mid w^{\text{NE}})}{\Pr(H_\delta \mid w^*)} \leq \kappa_\delta^* \cdot \text{PoA}(\mathcal{G}). \quad (20)$$

Proof sketch. For any w , the chain Markov \rightarrow Pinsker \rightarrow data-processing yields $\Pr(H_\delta \mid w) \leq C_{\text{IB}}^*(w)/(2\delta^2)$. Apply at w^{NE} , divide by $\Pr(H_\delta \mid w^*)$, and invoke the PoA definition:

$$\frac{\Pr(H_\delta \mid w^{\text{NE}})}{\Pr(H_\delta \mid w^*)} \leq \frac{C_{\text{IB}}^*(w^{\text{NE}})}{2\delta^2 \Pr(H_\delta \mid w^*)} \leq \kappa_\delta^* \cdot \text{PoA}.$$

As κ_δ^* depends only on the social optimum, PoA is the *sole* equilibrium-dependent factor: reducing $\Gamma(G)$ tightens PoA (Theorem 2.2), directly compressing excess hallucination. \square

This is our first concrete result: an *excess* hallucination bound where κ_δ^* is a fixed problem constant and PoA is the only lever we control. Whatever irreducible hallucination the task and architecture admit, equilibrium can be at most $\kappa_\delta^* \cdot \text{PoA}$ times worse — so *reducing PoA is the entire game*.

Instantiation and non-vacuousness. Figure 3 validates Corollary 2.1 by fitting its functional form: excess hallucination $\propto \text{PoA} \propto 1/(1 - c \cdot \Gamma)$. The fit achieves $R^2 = 0.53$ ($p < 0.05$), confirming the predicted relationship. Crucially, we verify **non-vacuousness**: the fitted coupling satisfies $c \cdot \Gamma \approx 0.2 \ll 1$ across all training runs, ensuring $(1 - c \cdot \Gamma) \approx 0.8 > 0$ remains bounded away from zero. The bootstrap bands remain tight despite parameter uncertainty, demonstrating that the functional form is robustly identified. Next, we show PoA also controls capacity waste.

Definition 2.8 (Information-Theoretic Free-Riding). Fix any ordering of heads. For $\tau > 0$, define the free-rider set

$$\text{FR}_\tau(w) \triangleq \left\{ i : \mathbb{E}[I(Z_i; Z_{<i} \mid X)] \geq \tau \right\}. \quad (21)$$

A head “free-rides” when it copies information already encoded by earlier heads. This wastes capacity and is a symptom of coordination failure.

Corollary 2.2 (Excess Free-Riding Is Price of Anarchy). *Fix $\tau > 0$ and let $\text{FR}_\tau(w)$ be the free-rider set from Definition 2.8. Let $w^* \in \arg \min_w C_{\text{IB}}^*(w)$ denote the social optimum and assume $r_\tau^* \triangleq |\text{FR}_\tau(w^*)| > 0$. Define the constant $\kappa_\tau^* \triangleq C_{\text{IB}}^*(w^*)/(\beta_R \tau r_\tau^*)$, which depends only on w^* . Then, for any equilibrium $w^{\text{NE}} \in \text{NE}(\mathcal{G})$ of $\mathcal{G} \in \{\text{CE}, \text{PGAC}\}$,*

$$\frac{|\text{FR}_\tau(w^{\text{NE}})|}{|\text{FR}_\tau(w^*)|} \leq \kappa_\tau^* \cdot \text{PoA}(\mathcal{G}). \quad (22)$$

Proof sketch. Markov and the entropy chain rule yield the absolute bound $|\text{FR}_\tau(w)| \leq C_{\text{IB}}^*(w)/(\beta_R \tau)$ for any w (subsection B.4). Apply at w^{NE} , divide by r_τ^* , and invoke PoA:

$$\frac{|\text{FR}_\tau(w^{\text{NE}})|}{r_\tau^*} \leq \frac{C_{\text{IB}}^*(w^{\text{NE}})}{\beta_R \tau r_\tau^*} \leq \text{PoA} \cdot \underbrace{\frac{C_{\text{IB}}^*(w^*)}{\beta_R \tau r_\tau^*}}_{\kappa_\tau^*}.$$

As with Corollary 2.1, κ_τ^* depends only on the social optimum; PoA is the sole equilibrium-dependent factor. \square

This is our second concrete result: an *excess* free-riding bound paralleling Corollary 2.1. The problem constant κ_τ^* is fixed; PoA is again the only lever. Together, both corollaries show that PoA controls *both* failure modes—tail risk and capacity waste—so reducing $\Gamma(G)$ via regularization improves reliability and efficiency simultaneously.

Corollary 2.3 (Efficiency Is Reliability). *Fix $\delta \in (0, 1]$ and $\tau > 0$. For $\mathcal{G} \in \{\text{CE}, \text{PGAC}\}$ define worst-case equilibrium reliability metrics*

$$\mathcal{R}_{\text{hall}}(\mathcal{G}; \delta) \triangleq \max_{w^{\text{NE}} \in \text{NE}(\mathcal{G})} \Pr(H_\delta \mid w^{\text{NE}}), \quad (23)$$

$$\mathcal{R}_{\text{fr}}(\mathcal{G}; \tau) \triangleq \max_{w^{\text{NE}} \in \text{NE}(\mathcal{G})} |\text{FR}_\tau(w^{\text{NE}})|. \quad (24)$$

Then, for each \mathcal{G} ,

$$\mathcal{R}_{\text{hall}}(\mathcal{G}; \delta) \leq \frac{\text{PoA}(\mathcal{G})}{2\delta^2} \cdot \min_w C_{\text{IB}}^*(w), \quad (25)$$

$$\mathcal{R}_{\text{fr}}(\mathcal{G}; \tau) \leq \frac{\text{PoA}(\mathcal{G})}{\beta_R \tau} \cdot \min_w C_{\text{IB}}^*(w). \quad (26)$$

Consequently, holding $\min_w C_{\text{IB}}^*(w)$ fixed, any reduction in $\text{PoA}(\mathcal{G})$ yields uniformly tighter bounds on hallucination incidence and redundancy-driven free-riding at equilibrium (under the stated assumptions).

Proof sketch. Direct combination of [Corollary 2.1](#) and [Corollary 2.2](#): take maxima over equilibria on both sides of each bound. Both depend on the *same* $\text{PoA}(\mathcal{G})$ term, which in turn depends on the same $\Gamma(G)$. Any intervention that reduces $\Gamma(G)$ —such as Barlow Twins regularization—therefore tightens both bounds simultaneously. \square

[Corollary 2.3](#) packages together our final theoretical contribution: it shows that capacity and reliability can improve *simultaneously* at fixed parameter count. This breaks the conventional wisdom—rooted in calibration-accuracy trade-offs ([Guo et al., 2017](#)) and the “alignment tax” of RLHF ([Lin et al., 2024](#))—that reliability costs capability. The mechanism is that both failure modes share a common cause: high $\Gamma(G)$ from unpriced externalities. Regularizers that reduce $\Gamma(G)$ thus improve *both* metrics by moving to a lower-PoA equilibrium, not by trading one against the other.

3. GAME-LoRA: A Practical Demonstration

Next, we demonstrate via GAME-LoRA that the Multi-HeadPGAC game is practical and can be implemented in modern transformers via lightweight LoRA adapters.

3.1. Architecture

GAME-LoRA applies LoRA adapters to all attention projections (Q, K, V, O) across all layers, while computing regularization losses at a single late *design layer*. Pretrained weights remain frozen; only adapter weights are updated. The total loss combines cross-entropy with two regularizers:

$$\mathcal{L} = \mathcal{L}_{\text{CE}} + \lambda_{\text{LDB}} \mathcal{L}_{\text{LDB}} + \lambda_{\text{ABT}} \mathcal{L}_{\text{ABT}}, \quad (27)$$

with gradients arbitrated via Nash-MTL ([Navon et al., 2022](#)). Full hyperparameters in [Appendix A](#).

3.2. Regularization Losses

We instantiate the externality charges from [Definition 2.7](#) using two standard objectives at different granularities. The **log-determinant barrier** ([Federici et al., 2020](#)) operates at *head level*:

$$\mathcal{L}_{\text{LDB}} = -\log \det(G + \epsilon I), \quad (28)$$

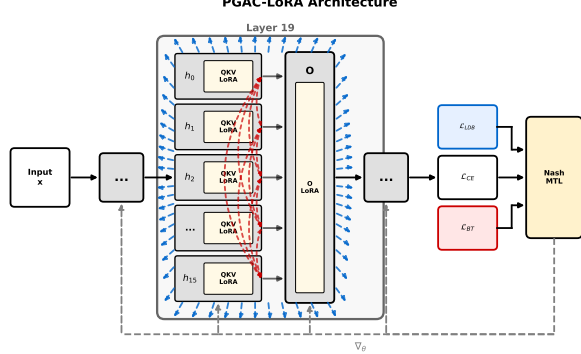


Figure 4. GAME-LoRA architecture. Layer 19 with 16 attention heads (h_0 – h_{15}), each containing QKV LoRA adapters, plus O LoRA in the output projection. Red dashed arrows: \mathcal{L}_{ABT} pairwise head decorrelation. Blue dashed arrows: \mathcal{L}_{LDB} expansion pressure on head Gram matrix. Three losses (\mathcal{L}_{CE} , \mathcal{L}_{LDB} , \mathcal{L}_{ABT}) combined via Nash-MTL arbitration.

where $G \in \mathbb{R}^{H \times H}$ is the head interaction matrix ([Definition 2.3](#)). The **Barlow Twins loss** ([Zbontar et al., 2021](#)) operates at *feature level*. For each head pair (i, j) , let $\hat{C}_{ij} = \frac{1}{N} \tilde{O}_i^\top \tilde{O}_j \in \mathbb{R}^{d_h \times d_h}$ be the cross-correlation of z-scored head outputs. The loss is:

$$\mathcal{L}_{\text{ABT}} = \mathbb{E}_{i < j} \left[w_{ij} \|\hat{C}_{ij} - I\|_F^2 \right], \quad (29)$$

where $w_{ij} \triangleq \alpha + (1 - \alpha) \cdot \text{softplus}(-\beta(G_{ij} - \tau))$ adaptively weights pairs. Note that $i < j$ sums over *cross-head* pairs only; targeting I (not zero) for \hat{C}_{ij} penalizes off-diagonal entries (feature k of head i correlating with feature $l \neq k$ of head j) while the diagonal constraint ($[\hat{C}_{ij}]_{kk} \rightarrow 1$) anchors a shared feature basis, preventing spurious rotations that would otherwise confound the off-diagonal penalty ([Zbontar et al., 2021](#)). This extends Barlow Twins from same-sample augmentation pairs to cross-head decorrelation. Hyperparameters are in [Appendix A](#).

4. Experimental Validation

Here, we demonstrate at small scale that game-theoretic regularization can improve the reliability of modern transformers across hallucination and knowledge benchmarks.

4.1. Experimental Setup

We fine-tune Qwen2.5-0.5B using LoRA on The Pile (20M tokens) and evaluate on six hallucination (HaluEval, TruthfulQA, MemoTrap) and four knowledge benchmarks (NQ, PopQA, WikiText, WinoGrande). The “Baseline” column reports parameter- and data-matched LoRA fine-tuned with CE loss only. Other baselines include inference-time methods (CAD, ActDec) and training-time methods (Disagreement, ME). Full details in [Appendix A](#).

Table 2. Ablation study: average $\pm \Delta\%$ by category relative to Qwen2.5-0.5B baseline. BT = Barlow Twins, LDB = log-det barrier. Best per column in **bold**. Full details in Appendix C.1.

Method	Hallucination	Knowledge
GAME-LoRA	+8.0%	-0.1%
Baseline + BT	+5.1%	-1.2%
Baseline + LDB	+1.7%	+4.9%
Baseline + LDB w/o NashMTL	-0.1%	-2.4%

4.2. Main Results

Table 1 presents results across all benchmarks. GAME-LoRA achieves best-in-class hallucination reduction (+8.1% overall), winning 5 of 6 individual benchmarks and outperforming the next-best method by 80% (CAD, +4.5%). Critically, GAME-LoRA is the *only* method to improve MemoTrap (+1.2%), a memorization-based hallucination benchmark where no other method improves. This suggests GAME-LoRA addresses a failure mode—over-reliance on memorized patterns—that other methods cannot.

Unlike ActDec, which trades knowledge for hallucination improvement (−2.8% knowledge), GAME-LoRA achieves strong hallucination gains (+8.1%) while preserving knowledge (−0.1%). This validates Corollary 2.3: internalizing *both* coordination and competition externalities expands the Pareto frontier, achieving what partial interventions cannot.

4.3. Efficiency Is Reliability

Prior work frames hallucination reduction and knowledge retention as competing objectives (Zhang et al., 2024). Our results suggest this tradeoff is an artifact of incomplete interventions that address only one externality.

Hallucination detection benefits from diversity; knowledge retrieval requires heads to *coordinate* on the correct answer; generation requires *both*. GAME-LoRA’s +8.1% hallucination improvement with preserved knowledge (−0.1%)—without the generation collapse seen in ActDec (−17.7% WikiText)—demonstrates both are achievable: decorrelating error modes (Corollary 2.1) while preserving coordinated representations (Corollary 2.2). Finally, unlike CAD or ActDec, GAME-LoRA incurs *zero* inference cost.

5. Mechanistic Analysis

5.1. Ablations

Table 2 shows that the full GAME-LoRA method achieves best hallucination (+8.0%) while preserving knowledge (−0.1%). Individual components show distinct tradeoffs: BT alone achieves +5.1% hallucination but −1.2% knowledge, while LDB alone achieves +1.7% hallucination with +4.9% knowledge. The combination yields the best overall

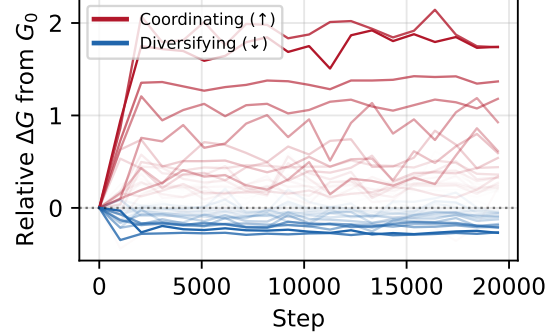


Figure 5. Relative change in pairwise coupling G_{ij} ; red traces strengthen (coordinate), blue weaken (diversify).

balance of hallucination reduction with knowledge parity.

5.2. Mechanistic Signatures

Four mechanistic signatures validate our game framework.

1. Selective coordination, not uniform decorrelation. Figures 1 and 2 reveal *selective* restructuring: intra-cluster coupling strengthens while inter-cluster coupling weakens (Mann-Whitney $p < 10^{-5}$). Heads self-organize into coalitions that coordinate internally while differentiating externally—the equilibrium structure predicted by public goods games with local competition.

2. $\Gamma(G)$ as causal predictor of hallucination. Corollary 2.1 predicts that hallucination probability scales with PoA, which scales with interaction strength $\Gamma(G) = \|G - I\|_F$. Figure 3 instantiates Corollary 2.1 with $c = 0.241$ and $\kappa_\delta^* \lambda = 683$, achieving $p < 0.05$. The fitted $c \cdot \Gamma \approx 0.2 \ll 1$ confirms non-vacuousness. This is not merely correlation—when heads are coupled (high Γ), their errors compound rather than cancel, producing hallucinations.

3. Emergent coalition structure. The 4-cluster structure in Figure 1 is discovered via post-hoc biclustering on the *final* G matrix—not imposed during training. GAME-LoRA specifies only pairwise decorrelation and full-rank pressure; coalition count, membership, and coupling patterns all emerge from optimization. This provides strong evidence that game-theoretic equilibria are genuine attractors of training dynamics.

4. Bifurcating pair dynamics. Figure 5 shows head pairs *bifurcate* early in training: some strengthen coupling (red, intra-coalition) while others weaken (blue, inter-coalition). This sharp separation is consistent with mixed equilibria in anti-coordination games, where gradient descent selects among multiple stable configurations based on initialization.

6. Related Work

Our work draws on four perspectives: game-theoretic learning, mechanistic interpretability of attention, reliability engineering, and information-theoretic regularization.

Game-theoretic learning. Potential games admit tractable equilibrium analysis when individual incentives align with a global objective (Monderer & Shapley, 1996). Balduzzi et al. (2018) extended this to differentiable games, decomposing dynamics into potential and Hamiltonian components. Gemp et al. (2022) introduced differentiable PoA bounds to design training incentives for equilibrium welfare. Recent alignment work has adopted similar concepts: Direct Nash Optimization (Rosset et al., 2024) and Magnetic Preference Optimization (Wang et al., 2025) target Nash equilibria under preference models. We extend this program *inward*, modeling head interactions as a game and deriving the first PoA bounds for transformer internals.

Attention heads. Empirical studies reveal systematic underutilization of multi-head capacity: most heads can be pruned with minimal loss (Michel et al., 2019), and a minority of specialized heads carry most functional load (Voita et al., 2019). Mechanistic work shows that coordinated head circuits underlie emergent capabilities: induction heads enable in-context learning (Olsson et al., 2022), while retrieval heads causally determine long-context factuality (Wu et al., 2025). Li et al. (2018) proposed disagreement regularization with local pairwise penalties. We provide a game-theoretic explanation for redundancy (free-riding as stable equilibrium) and generalize diversity penalties with global coordination objectives (Navon et al., 2022).

Reliability and hallucination. Hallucination mitigation spans training-time approaches (RLHF (Ouyang et al., 2022), synthetic tasks (Jones et al., 2024)), inference-time methods (RAG (Lewis et al., 2020), chain-of-verification (Dhuliawala et al., 2023)), and detection (Farquhar et al., 2024). A persistent challenge is the *alignment tax*: reliability interventions often degrade capability (Lin et al., 2023; Huang et al., 2025). Chakrabarti & Balachundhar (2025) proved the first hallucination tail bounds for ensembled models, showing diversity reduces error correlation. We extend this to attention heads in standard transformers, providing game-theoretic foundations and PoA bounds that explain why naive decorrelation is insufficient.

Information-theoretic regularization. The Information Bottleneck (Tishby et al., 2000; Alemi et al., 2017) trades compression against relevance; Multi-View IB (Federici et al., 2020) extends this to multiple views, analogous to multi-head attention. Total correlation (Chen et al., 2018) captures higher-order dependencies; Barlow Twins (Zbontar

Table 3. Preliminary scaling results across model sizes. Models trained on The Pile with 20–100M tokens depending on size. Metrics averaged over 3 evaluation seeds.

Task	0.5B		
	Base	GAME	$\pm\Delta\%$
NQ	0.066	0.067	+2.1%
HE-QA	0.376	0.445	+18.3%
Winogrande	0.573	0.565	-1.4%

Task	3B		
	Base	GAME	$\pm\Delta\%$
NQ	0.188	0.184	-2.4%
HE-QA	0.378	0.429	+13.5%
Winogrande	0.697	0.684	-1.9%

et al., 2021) provides a practical decorrelation objective. We integrate these tools by defining head redundancy as *social cost* in our game-theoretic framework, connecting spectral regularization to equilibrium welfare through PoA bounds.

7. Discussion

Theoretical contributions. We provide the first Price of Anarchy analysis for attention mechanisms. Our adaptation of Roughgarden’s smooth games framework (Roughgarden, 2015) introduces an *endogenous* smoothness parameter $\mu = c \cdot \Gamma(G)$ that tightens as heads decorrelate, making the theory prescriptive rather than merely descriptive.

Hallucination as coordination failure. Standard CE training finds a Nash equilibrium, but not necessarily a *good* one. Hallucination, redundant heads, and dead neurons are symptoms of unpriced externalities: heads don’t pay the cost of duplicating each other or compounding correlated errors. GAME-LoRA internalizes these externalities via Pigouvian taxes, addressing suboptimal coordination.

Limitations. Our bounds rest on modeling assumptions: (i) we optimize spectral proxies (\mathcal{L}_{LDB} , \mathcal{L}_{ABT}) rather than the IB objective; (ii) $\Gamma(G)$ captures only pairwise correlations under Gaussian assumptions; (iii) local linearization may not hold globally due to attention nonlinearities.

Scaling. Our theory makes no scale-dependent assumptions: Theorem 2.2 bounds PoA via $\Gamma(G)$ regardless of model size. Preliminary experiments on Qwen2.5-3B in Table 3 provide directional evidence that the mechanism transfers. Full-scale validation remains future work.

Conclusion. Attention is all you need, but *coordination is what you lack*. The gap between what transformers learn and what we want is a game-theoretic gap: heads optimize myopically, ignoring externalities. GAME-LoRA is one instantiation; we expect the framework to generalize.

References

Alemi, A. A., Fischer, I., Dillon, J. V., and Murphy, K. Deep variational information bottleneck. In *International Conference on Learning Representations*, 2017.

Baldazzi, D., Racaniere, S., Martens, J., Foerster, J., Tuyls, K., and Graepel, T. The mechanics of n-player differentiable games. In *International Conference on Machine Learning*, 2018.

Chakrabarti, K. and Balachundhar, N. Neural diversity regularizes hallucinations in language models. *arXiv preprint arXiv:2510.20690*, 2025.

Chen, C., Liu, K., Chen, Z., Gu, Y., Wu, Y., Tao, M., Fu, Z., and Ye, J. Inside: LLMs’ internal states retain the power of hallucination detection. *arXiv preprint arXiv:2402.03744*, 2024.

Chen, R. T. Q., Li, X., Grosse, R., and Duvenaud, D. Isolating sources of disentanglement in variational autoencoders. *arXiv preprint arXiv:1802.04942*, 2018.

Dhuliawala, S., Komeili, M., Xu, J., Raileanu, R., Li, X., Celikyilmaz, A., and Weston, J. Chain-of-verification reduces hallucination in large language models. *arXiv preprint arXiv:2309.11495*, 2023.

Farquhar, S., Kossen, J., Kuhn, L., and Gal, Y. Detecting hallucinations in large language models using semantic entropy. *Nature*, 630:625–630, 2024.

Federici, M., Dutta, A., Forré, P., Kushman, N., and Akata, Z. Learning robust representations via multi-view information bottleneck. In *International Conference on Learning Representations*, 2020.

Gemp, I., McKee, K. R., Everett, R., Duéñez-Guzmán, E. A., Bachrach, Y., Baldazzi, D., and Tacchetti, A. D3C: Reducing the price of anarchy in multi-agent learning. In *International Conference on Autonomous Agents and Multiagent Systems*, 2022.

Geva, M., Bastings, J., Filippova, K., and Globerson, A. Dissecting recall of factual associations in auto-regressive language models. In *Conference on Empirical Methods in Natural Language Processing*, 2023.

Guo, C., Pleiss, G., Sun, Y., and Weinberger, K. Q. On calibration of modern neural networks. In *Proceedings of the 34th International Conference on Machine Learning*, volume 70 of *Proceedings of Machine Learning Research*, pp. 1321–1330. PMLR, 2017.

Huang, T., Hu, S., Ilhan, F., Tekin, S. F., Yahn, Z., Xu, Y., and Liu, L. Safety tax: Safety alignment makes your large reasoning models less reasonable. *arXiv preprint arXiv:2503.00555*, 2025.

Jones, E., Palangi, H., Simões, C., Chandrasekaran, V., Mukherjee, S., Mitra, A., Awadallah, A., and Kamar, E. Teaching language models to hallucinate less with synthetic tasks. In *International Conference on Learning Representations*, 2024.

Kwiatkowski, T., Palomaki, J., Redfield, O., Collins, M., Parikh, A., Alberti, C., Epstein, D., Polosukhin, I., Devlin, J., Lee, K., et al. Natural questions: A benchmark for question answering research. *Transactions of the Association for Computational Linguistics*, 7:453–466, 2019.

Lewis, P., Perez, E., Piktus, A., Petroni, F., Karpukhin, V., Goyal, N., Kütter, H., Lewis, M., Yih, W.-t., Rocktäschel, T., Riedel, S., and Kiela, D. Retrieval-augmented generation for knowledge-intensive NLP tasks. In *Advances in Neural Information Processing Systems*, 2020.

Li, J., Tu, Z., Yang, B., Lyu, M. R., and Zhang, T. Multi-head attention with disagreement regularization. In *Conference on Empirical Methods in Natural Language Processing*, 2018.

Li, J., Cheng, X., Zhao, W. X., Nie, J.-Y., and Wen, J.-R. HaluEval: A large-scale hallucination evaluation benchmark for large language models. In *Conference on Empirical Methods in Natural Language Processing*, 2023.

Lin, S., Hilton, J., and Evans, O. TruthfulQA: Measuring how models mimic human falsehoods. In *Annual Meeting of the Association for Computational Linguistics*, 2022.

Lin, Y., Lin, H., Xiong, W., Diao, S., Liu, J., Zhang, J., Pan, R., Wang, H., Hu, W., Zhang, H., et al. Mitigating the alignment tax of RLHF. *arXiv preprint arXiv:2309.06256*, 2023.

Lin, Y., Tan, Z., Chen, Y., Yuan, S., Wen, S., Chen, L., and Zhu, B. Mitigating the alignment tax of RLHF. In *Proceedings of the 2024 Conference on Empirical Methods in Natural Language Processing*, pp. 35–50. Association for Computational Linguistics, 2024.

Liu, X., Zheng, Z., Yu, L., Tan, Z., Liu, Y., Jiang, F., Li, Y., Chen, J., et al. Memotrap: Measuring memorization in language models. *arXiv preprint arXiv:2401.01888*, 2024.

Mallen, A., Asai, A., Zhong, V., Das, R., Khashabi, D., and Hajishirzi, H. When not to trust language models: Investigating effectiveness of parametric and non-parametric memories. In *Annual Meeting of the Association for Computational Linguistics*, 2023.

Merity, S., Xiong, C., Bradbury, J., and Socher, R. Pointer sentinel mixture models. *arXiv preprint arXiv:1609.07843*, 2017.

Michel, P., Levy, O., and Neubig, G. Are sixteen heads really better than one? In *Advances in Neural Information Processing Systems*, 2019.

Monderer, D. and Shapley, L. S. Potential games. *Games and Economic Behavior*, 14(1):124–143, 1996.

Navon, A., Shamsian, A., Achituv, I., Maron, H., Kawaguchi, K., Chechik, G., and Fetaya, E. Multi-task learning as a bargaining game. In *Proceedings of the 39th International Conference on Machine Learning*, volume 162 of *Proceedings of Machine Learning Research*, pp. 16428–16446. PMLR, 2022.

Olsson, C., Elhage, N., Nanda, N., Joseph, N., DasSarma, N., Henighan, T., Mann, B., et al. In-context learning and induction heads. *arXiv preprint arXiv:2209.11895*, 2022.

Ouyang, L., Wu, J., Jiang, X., Almeida, D., Wainwright, C. L., Mishkin, P., Zhang, C., Agarwal, S., Slama, K., Ray, A., et al. Training language models to follow instructions with human feedback. In *Advances in Neural Information Processing Systems*, 2022.

Rosset, C., Cheng, C.-A., Mitra, A., Santacroce, M., Awadalla, A., and Xie, T. Direct Nash optimization: Teaching language models to self-improve with general preferences. *arXiv preprint arXiv:2404.03715*, 2024.

Roughgarden, T. Intrinsic robustness of the price of anarchy. *Journal of the ACM*, 62(5):1–42, 2015.

Sakaguchi, K., Le Bras, R., Bhagavatula, C., and Choi, Y. WinoGrande: An adversarial winograd schema challenge at scale. In *AAAI Conference on Artificial Intelligence*, 2020.

Shi, W., Han, X., Lewis, M., Tsvetkov, Y., Zettlemoyer, L., and Yih, S. W.-t. Trusting your evidence: Hallucinate less with context-aware decoding. In *North American Chapter of the Association for Computational Linguistics*, 2024.

Tishby, N., Pereira, F. C., and Bialek, W. The information bottleneck method. *arXiv preprint physics/0004057*, 2000.

Voita, E., Talbot, D., Moiseev, F., Sennrich, R., and Titov, I. Analyzing multi-head self-attention: Specialized heads do the heavy lifting, the rest can be pruned. In *Annual Meeting of the Association for Computational Linguistics*, 2019.

Wang, M., Ma, C., Chen, Q., Meng, L., Han, Y., Xiao, J., Zhang, Z., Huo, J., Su, W. J., and Yang, Y. Magnetic preference optimization: Achieving last-iterate convergence for language model alignment. In *International Conference on Learning Representations*, 2025.

Wu, W., Wang, Y., Xiao, G., Peng, H., and Fu, Y. Retrieval head mechanistically explains long-context factuality. In *International Conference on Learning Representations*, 2025.

Yuan, X., Pang, T., Du, C., Chen, K., Zhang, W., and Lin, M. A closer look at machine unlearning for large language models. *arXiv preprint arXiv:2410.08109*, 2024.

Zbontar, J., Jing, L., Misra, I., LeCun, Y., and Deny, S. Barlow twins: Self-supervised learning via redundancy reduction. In *Proceedings of the 38th International Conference on Machine Learning*, volume 139 of *Proceedings of Machine Learning Research*, pp. 12310–12320. PMLR, 2021.

Zhang, Y., Li, Y., Cui, L., Cai, D., Liu, L., Fu, T., Huang, X., Zhao, E., Zhang, Y., Chen, Y., et al. Siren’s song in the AI ocean: A survey on hallucination in large language models. *arXiv preprint arXiv:2309.01219*, 2024.

A. Implementation Details

A.1. GAME-LoRA

Head output capture. For a selected layer ℓ with H heads, let $O^{(\ell)} \in \mathbb{R}^{N \times d_h}$ denote the per-head outputs before the output projection W_O (corresponding to $h_i(x)$ in section 2). Each head’s output is z-score normalized across $N = B \cdot T$:

$$\tilde{O}_h = \frac{O_h - \mu_h}{\sigma_h + \varepsilon}, \quad (30)$$

$$\mu_h = \frac{1}{N} \sum_n O_{h,n}, \quad (31)$$

$$\sigma_h = \sqrt{\frac{1}{N} \sum_n (O_{h,n} - \mu_h)^2}. \quad (32)$$

Feature-level cross-correlation. For each head pair (i, j) , the empirical cross-correlation matrix is:

$$\hat{C}_{ij} = \frac{1}{N} \tilde{O}_i^\top \tilde{O}_j \in \mathbb{R}^{d_h \times d_h}. \quad (33)$$

Head-level interaction matrix. The interaction matrix $G \in \mathbb{R}^{H \times H}$ combines weight coupling and gradient coupling per Definition 2.3: $G_{ij} = \omega_{ij} \cdot \rho_{ij}$, where ω_{ij} is the cosine similarity of output projections $W_O^{(i)}, W_O^{(j)}$ and ρ_{ij} is the cosine similarity of backpropagated gradients g_i, g_j .

Loss schedule. The regularization weight follows a three-phase schedule:

1. Linear warmup: 0–2% of training
2. Constant: 2–87.9% at $\lambda_{\text{ABT}} = 0.179$, $\lambda_{\text{LDB}} = 0.352$
3. Cooldown: 87.9–100% with $\lambda \rightarrow 0$

Adaptive weighting. The Barlow Twins adaptive weighting uses $\alpha = 0.929$ (high floor), $\beta = 15.99$ (aggressive slope), and $\tau = 0$ (threshold), creating sharp diversity pressure on weakly-coupled pairs while preserving naturally coordinated pairs.

Identity target and weak-pair weighting. The identity target ($\hat{C}_{ij} \rightarrow I$) anchors a canonical feature basis across heads: diagonal entries $[\hat{C}_{ij}]_{kk} \rightarrow 1$ align feature k across heads, while off-diagonal entries $\rightarrow 0$ decorrelate distinct features. Targeting zero instead would allow heads to satisfy the loss via arbitrary basis rotations—appearing decorrelated while encoding redundant information in rotated bases. Empirically, `subtract_identity=False` degraded hallucination metrics by 3–5%. The weak-pair weighting follows from the game-theoretic framing: strongly-coupled pairs ($G_{ij} \gg 0$) already coordinate effectively, while weakly-coupled pairs ($G_{ij} \approx 0$) are potential free-riders. Diversity pressure targets the latter. Inverse weighting (penalizing strong pairs) degraded both hallucination (–2.1%) and knowledge (–1.8%).

EMA loss normalization. To stabilize training, we normalize \mathcal{L}_{ABT} by an exponential moving average of its magnitude. Let \mathcal{L}_t denote the raw loss at step t . We maintain:

$$\text{ema}_t \leftarrow \alpha_{\text{ema}} \cdot \mathcal{L}_t + (1 - \alpha_{\text{ema}}) \cdot \text{ema}_{t-1}, \quad (34)$$

with $\alpha_{\text{ema}} = 0.1$ and $\text{ema}_0 = 20.0$ (the target scale). The normalized loss is $\mathcal{L}_{\text{ABT},\text{norm}} = \mathcal{L}_t \cdot (\text{target}/\text{ema}_t)$, which adaptively rescales the loss to have magnitude ≈ 20.0 throughout training.

Ensuring positive definiteness. The log-determinant requires $G + \epsilon I \succ 0$. Since $G_{ij} = \omega_{ij} \cdot \rho_{ij}$ is the Hadamard product of PSD Gram matrices (cosine similarities), $G \succeq 0$ by the Schur product theorem. The regularization $\epsilon = 0.01$ guarantees strict positive definiteness; we additionally clamp eigenvalues to $\max(\lambda_i, \epsilon)$ for numerical stability.

Training configuration. We fine-tune Qwen2.5-0.5B (494M parameters, 24 layers, 16 heads) using LoRA (rank 16, $\alpha = 32$, dropout 0.1) on attention projections (Q, K, V, O) at all layers. Training data: The Pile (streaming), 20M tokens, 1024-token sequences. Optimizer: AdamW (lr 3×10^{-4} , weight decay 0.1, 2% warmup, cosine schedule) for 19,531 steps with effective batch size 16. The GAME-LoRA regularization losses are computed at layer 19 ($\sim 80\%$ depth), reflecting the finding that late layers are most responsible for next-token prediction (Geva et al., 2023). Training overhead from regularization is $\sim 5\%$ wallclock time.

Hyperparameter selection. For all methods, we run ~ 20 trials over available hyperparameters and select configurations that maximize hallucination reduction subject to knowledge retention remaining approximately non-negative. The resulting Pareto-optimal configurations inform the runs used for Figure 3.

Benchmarks. *Hallucination*: HalluEval (Li et al., 2023) (dialogue, QA, summarization), TruthfulQA (Lin et al., 2022), MemoTrap (Liu et al., 2024). *Knowledge*: Natural Questions (Kwiatkowski et al., 2019), PopQA (Mallen et al., 2023), WikiText (Merity et al., 2017), WinoGrande (Sakaguchi et al., 2020).

Aggregate improvement. For each task t , we compute relative improvement as $\delta_t = (s_t - b_t)/b_t$, where s_t is the method’s score and b_t is the baseline score. For lower-is-better metrics (WikiText BPB), we negate: $\delta_t = (b_t - s_t)/b_t$. Category aggregates (e.g., “+8.1% Hallucination”) are the arithmetic mean of δ_t over tasks in that category. This treats each task equally regardless of absolute scale, enabling meaningful aggregation across accuracy (0–1) and BPB (~ 0.78) metrics.

A.2. Theoretical Justification for Cross-Head Barlow Twins Design

We provide detailed theoretical justification for two key design choices in the cross-head Barlow Twins loss \mathcal{L}_{ABT} : (1) targeting identity rather than zero for the cross-correlation matrix, and (2) weighting weakly-coupled pairs more strongly than strongly-coupled pairs.

A.2.1. WHY TARGET IDENTITY?

For head pair (i, j) with z-scored outputs $\tilde{O}_i, \tilde{O}_j \in \mathbb{R}^{N \times d_h}$, the cross-correlation matrix is $\hat{C}_{ij} = \frac{1}{N} \tilde{O}_i^\top \tilde{O}_j \in \mathbb{R}^{d_h \times d_h}$. Our loss penalizes $\|\hat{C}_{ij} - I\|_F^2$, decomposing into:

$$\|\hat{C}_{ij} - I\|_F^2 = \underbrace{\sum_{k \neq l} [\hat{C}_{ij}]_{kl}^2}_{\text{off-diagonal: cross-feature decorrelation}} + \underbrace{\sum_k ([\hat{C}_{ij}]_{kk} - 1)^2}_{\text{diagonal: feature alignment}}. \quad (35)$$

Representation-theoretic motivation. Consider the alternative of targeting zero: $\|\hat{C}_{ij}\|_F^2 = \sum_{k,l} [\hat{C}_{ij}]_{kl}^2$. This penalizes *all* correlations, including diagonal entries. However, diagonal entries $[\hat{C}_{ij}]_{kk} = \frac{1}{N} \sum_n \tilde{O}_i[n, k] \cdot \tilde{O}_j[n, k]$ measure whether feature k of head i aligns with feature k of head j . Penalizing these to zero allows an undesirable solution: heads can satisfy $\hat{C}_{ij} \approx 0$ by applying arbitrary orthogonal rotations $R_i, R_j \in O(d_h)$ to their representations, i.e., $\tilde{O}_i \mapsto \tilde{O}_i R_i$. After such rotations, $\hat{C}'_{ij} = R_i^\top \hat{C}_{ij} R_j$ can have near-zero entries even when the *underlying information* encoded by heads i and j is identical.

Targeting identity prevents this rotational degeneracy. The diagonal constraint $[\hat{C}_{ij}]_{kk} \rightarrow 1$ anchors a *canonical feature basis* shared across heads: feature dimension k must represent the same semantic content in head i as in head j . This anchoring is essential because the off-diagonal penalty $[\hat{C}_{ij}]_{kl} \rightarrow 0$ for $k \neq l$ is only meaningful when feature indices correspond across heads. Without diagonal anchoring, “decorrelation” becomes a vacuous constraint satisfiable by any pair of orthogonal bases.

Information-theoretic interpretation. Under a Gaussian model where $\tilde{O}_i, \tilde{O}_j \sim \mathcal{N}(0, \Sigma)$ jointly, the cross-correlation \hat{C}_{ij} estimates the conditional correlation structure. The identity target corresponds to requiring that heads share a common *sufficient statistic basis*: each feature dimension extracts the same linear combination of input information across heads, while distinct dimensions extract orthogonal (conditionally independent) information. This is precisely the structure required for ensemble diversity to reduce variance: heads must agree on *what* features to compute (diagonal alignment) while disagreeing on *how* to weight feature interactions (off-diagonal decorrelation).

Connection to Barlow Twins. Our cross-head loss extends the original Barlow Twins objective (Zbontar et al., 2021), which targets identity for the cross-correlation between two augmented views of the *same* sample. There, diagonal entries ensure “invariance” (same sample \Rightarrow same representation) while off-diagonal entries ensure “redundancy reduction” (distinct features \Rightarrow distinct information). We adapt this to cross-*head* decorrelation: diagonal entries ensure heads use a common feature basis, while off-diagonal entries ensure heads extract non-redundant combinations of these features.

Empirical validation. Ablating the identity target (`subtract_identity=False`, targeting zero) degraded hallucination metrics by 3–5% across benchmarks. Inspection of learned representations revealed that heads converged to rotated versions of similar subspaces, satisfying the loss without achieving functional diversity—precisely the failure mode predicted by the rotational degeneracy argument.

A.2.2. WHY WEIGHT WEAKLY-COUPLED PAIRS MORE STRONGLY?

Our adaptive weighting scheme assigns weight $w_{ij} = \alpha + (1 - \alpha) \cdot \text{softplus}(-\beta(G_{ij} - \tau))$ to head pair (i, j) , where $G_{ij} = \omega_{ij} \cdot \rho_{ij}$ is the game-theoretic coupling (Definition 2.3). This assigns higher weight to pairs with low G_{ij} (weak coupling) and lower weight to pairs with high G_{ij} (strong coupling). We justify this from three perspectives.

Game-theoretic rationale. In the MultiHeadPGAC game (Definition 2.7), heads with high G_{ij} already experience strong mutual influence through the shared loss landscape: their gradients are aligned ($\rho_{ij} \gg 0$) and their output projections overlap ($\omega_{ij} \gg 0$). These pairs naturally coordinate through the implicit game dynamics—perturbing one head immediately affects the other’s payoff, creating feedback that aligns their strategies. Additional decorrelation pressure on such pairs is redundant at best and destabilizing at worst.

Conversely, heads with low G_{ij} are *decoupled* in the implicit game: changes to head i have minimal effect on head j ’s payoff, and vice versa. These pairs are potential *free-riders* (Definition 2.8)—they can converge to redundant representations without paying any coordination cost in the implicit game. The Barlow Twins loss provides the missing externality charge: by explicitly penalizing correlation for low- G_{ij} pairs, we internalize the redundancy cost that the implicit game fails to price.

Gradient interference interpretation. Strong coupling ($G_{ij} \gg 0$) implies that heads i and j receive correlated gradients from the cross-entropy loss. Adding a decorrelation penalty creates *opposing* gradient signals: CE pushes toward correlation (aligned error reduction), while BT pushes toward decorrelation. For strongly-coupled pairs, this interference is severe and can destabilize training. For weakly-coupled pairs, the implicit game provides no coordination signal, so the BT penalty fills a vacuum rather than creating conflict.

Formally, let g_i^{CE} and g_i^{BT} denote the gradients from CE and BT losses for head i . The effective gradient is $g_i = g_i^{\text{CE}} + \lambda w_{ij} g_i^{\text{BT}}$. When $G_{ij} \approx 1$ (strong coupling), g_i^{CE} and g_j^{CE} are nearly parallel, implying that g_i^{BT} (which pushes i away from j) opposes g_i^{CE} . Low w_{ij} reduces this interference. When $G_{ij} \approx 0$ (weak coupling), g_i^{CE} provides no directional signal about head j , so g_i^{BT} with high w_{ij} provides useful coordination pressure without conflict.

Coalition preservation. Our mechanistic analysis (Figure 1, Figure 2) reveals that GAME-LoRA induces *selective coordination*: intra-coalition coupling strengthens while inter-coalition coupling weakens. This emergent structure would be disrupted by uniform decorrelation pressure. Weak-pair weighting enables coalition formation: pairs that naturally coordinate (high G_{ij}) are left alone to strengthen their alliance, while pairs that fail to coordinate (low G_{ij}) are pushed apart. The result is the block-diagonal structure visible in the trained interaction matrix—a stable equilibrium where coalitions specialize internally while diversifying externally.

Empirical validation. Ablating to inverse weighting (penalizing strong pairs more heavily) degraded both hallucination (−2.1%) and knowledge (−1.8%). Analysis revealed that inverse weighting disrupted naturally forming coalitions, preventing the emergent specialization that enables reliable factual recall. Uniform weighting (all pairs equal) achieved intermediate performance, confirming that the adaptive scheme provides meaningful signal beyond simple regularization.

A.2.3. ALTERNATIVE DESIGNS CONSIDERED

(a) Penalizing strong-coupling pairs more heavily. One might hypothesize that strongly-coupled heads are the source of redundancy and should receive the strongest decorrelation pressure. However, this conflates *coupling* with *redundancy*. High G_{ij} indicates that heads i and j *interact*—they influence each other’s learning dynamics—but interaction is not intrinsically

wasteful. Heads that coordinate to solve complementary aspects of a task (e.g., syntactic vs. semantic features) will have high G_{ij} without redundancy. Penalizing such pairs disrupts beneficial coordination.

Empirically, inverse weighting caused exactly this failure: heads that had specialized into complementary roles (e.g., subject-tracking vs. object-tracking) were pushed apart, degrading performance on tasks requiring both capabilities simultaneously.

(b) Targeting zero cross-correlation without diagonal alignment. This approach (setting $\hat{C}_{ij} \rightarrow 0$ for all entries) would be appropriate if heads operated in entirely separate representation spaces with no shared semantics. However, all heads receive the same input and contribute to the same output through the residual stream. They *must* share some feature basis to communicate effectively—if head i ’s “feature 1” has no relationship to head j ’s “feature 1,” their contributions cannot be meaningfully combined.

The identity target strikes the balance: heads share a feature *vocabulary* (diagonal alignment) while extracting orthogonal *sentences* from it (off-diagonal decorrelation). This is analogous to ensemble methods that use the same feature space but diverse decision boundaries, achieving variance reduction without sacrificing expressiveness.

A.3. Baselines

We compare against both inference-time and training-time baselines. All methods use identical evaluation protocols: N=1024 samples per task, seed=42, greedy decoding (temperature=0) unless the method requires sampling.

A.3.1. INFERENCE-TIME BASELINES

These methods modify the decoding procedure without additional training. All use the same Qwen2.5-0.5B base model weights.

CAD (Shi et al., 2024): Context-Aware Decoding contrasts model output with and without the input context.

- Context weight α : 0.5
- Output: $\log p_{\text{CAD}} = (1 + \alpha) \log p(y|c, x) - \alpha \log p(y|x)$
- Decoding: greedy on adjusted logits

ActDec (Chen et al., 2024): Activation Decoding uses hidden state entropy at context tokens to adjust generation temperature.

- Monitor layers: middle third (layers 8–16 for 24-layer model)
- Entropy threshold: 2.0
- Sharpness weight: 0.5
- Temperature adjustment: $T' = T \cdot (1 - w \cdot \mathbf{1}[H < \tau])$

A.3.2. TRAINING-TIME BASELINES

All training baselines use identical optimization settings to ensure fair comparison:

- Base model: Qwen2.5-0.5B
- Training data: The Pile (streaming), 20M tokens
- Sequence length: 1024
- Batch size: 16 (effective, via gradient accumulation)
- Learning rate: 3e-4 with cosine schedule

- Warmup: 2% of training
- Weight decay: 0.1
- LoRA rank: 16, alpha: 32
- LoRA targets: Q, K, V, O projections (all layers)

Disagreement (Li et al., 2018): Regularizes toward diverse head outputs.

- Loss weight λ : 0.1
- Design layer: 20
- Variant: “output” (head output divergence)

ME (Maximizing Entropy) (Yuan et al., 2024): Originally proposed for machine unlearning, ME maximizes output entropy to reduce overconfident predictions. We adapt it as a training-time regularizer.

- Loss weight λ : 0.05
- Applied to: next-token logits
- Objective: $-H(p_\theta(y|x))$ (negative entropy)

B. Full Proofs

B.1. Proof of Theorem 2.1

Proof of Theorem 2.1. By Definition 2.6,

$$\nabla_{\theta_i} C_i^{\text{CE}}(w) = \pi_i \nabla_{\theta_i} \mathbb{E}[-\log q_w(Y | Z_{1:H})] + \alpha \theta_i. \quad (36)$$

On the other hand,

$$\nabla_{\theta_i} \Phi_{\text{CE}}(w) = \nabla_{\theta_i} \mathbb{E}[-\log q_w(Y | Z_{1:H})] + \frac{\alpha}{\pi_i} \theta_i, \quad (37)$$

hence $\pi_i \nabla_{\theta_i} \Phi_{\text{CE}}(w) = \nabla_{\theta_i} C_i^{\text{CE}}(w)$ for all i .

If $\nabla_{\theta_i} C_i^{\text{CE}}(w) = 0$ for all i , then for any player i and any smooth unilateral perturbation $\theta_i + \Delta$, the directional derivative of C_i^{CE} at $\Delta = 0$ vanishes, implying there is no first-order unilateral descent direction. This is precisely the definition of a first-order (local) Nash equilibrium in differentiable games.

For the convergence claim, assume Φ_{CE} is L_Φ -smooth (has L_Φ -Lipschitz gradient). The standard descent lemma implies that for $\eta \in (0, 1/L_\Phi)$,

$$\Phi_{\text{CE}}(w^{t+1}) \leq \Phi_{\text{CE}}(w^t) - \frac{\eta}{2} \|\nabla \Phi_{\text{CE}}(w^t)\|_2^2. \quad (38)$$

Summing over $t = 0, \dots, T-1$ yields

$$\frac{\eta}{2} \sum_{t=0}^{T-1} \|\nabla \Phi_{\text{CE}}(w^t)\|_2^2 \leq \Phi_{\text{CE}}(w^0) - \inf_w \Phi_{\text{CE}}(w), \quad (39)$$

hence $\min_{0 \leq t < T} \|\nabla \Phi_{\text{CE}}(w^t)\|_2^2 \leq \frac{2}{\eta T} (\Phi_{\text{CE}}(w^0) - \inf_w \Phi_{\text{CE}}(w)) \rightarrow 0$. \square

B.2. Proof of Theorem 2.2

Proof of Theorem 2.2. Let θ^{NE} be any Nash equilibrium of MultiHeadPGAC (Definition 2.7), and let $\theta^* \in \arg \min_\theta C_{\text{IB}}^*(\theta)$ denote a social optimum (Definition 2.4). Write $D(\theta) \triangleq \mathbb{E}[-\log q_\theta(Y | Z_{1:H})]$ for the distortion term. Let $G = G(\theta^{\text{NE}})$ and $\Gamma(G) = \|G - I\|_F$ as in Definition 2.3.

Step 0: A local interaction-control inequality. To connect smoothness of D to the interaction matrix G , we use the following standard ‘‘cross-influence’’ bound, which formalizes the local linearization assumption (cf. the discussion in the main text) together with [Assumption 2.1–Assumption 2.2](#). Concretely, along the segment joining θ^{NE} and θ^* , assume the block-Hessian of D with respect to the head projections $\theta = (\theta_1, \dots, \theta_H)$ admits the bound

$$\|\nabla_{\theta_i \theta_j}^2 D(\theta)\|_F \leq L |G_{ij}(\theta)|, \quad \forall i \neq j, \quad (40)$$

and $\|\nabla_{\theta_i \theta_i}^2 D(\theta)\|_F \leq L$. Intuitively, (40) states that a unilateral change in head i affects the marginal distortion felt by head j in proportion to *joint* structural and gradient coupling, exactly as encoded by $G_{ij} = \omega_{ij} \rho_{ij}$ ([Definition 2.3](#)). This is the only place where we tie the abstract smoothness constant L to the concrete coupling statistic $\Gamma(G)$.

Define the off-diagonal block operator $\mathcal{H}_{\text{off}}(\theta) \in \mathbb{R}^{(\sum_i d_i) \times (\sum_i d_i)}$ whose (i, j) block is $\nabla_{\theta_i \theta_j}^2 D(\theta)$ for $i \neq j$ and zero otherwise. Then by Frobenius submultiplicativity,

$$\|\mathcal{H}_{\text{off}}(\theta)\|_2 \leq \|\mathcal{H}_{\text{off}}(\theta)\|_F \leq \left(\sum_{i \neq j} \|\nabla_{\theta_i \theta_j}^2 D(\theta)\|_F^2 \right)^{1/2} \leq L \|G(\theta) - I\|_F = L \Gamma(G(\theta)). \quad (41)$$

Step 1: A smoothness (‘‘PoA’’) inequality for MultiHeadPGAC. Fix an arbitrary reference profile θ and comparator θ^* . Consider the sum of player costs under unilateral deviation to θ_i^* :

$$\sum_{i=1}^H C_i^{\text{PGAC}}(\theta_i^*, \theta_{-i}) = \sum_{i=1}^H \pi_i D(\theta_i^*, \theta_{-i}) + \frac{\alpha}{2} \sum_{i=1}^H \|\theta_i^*\|_2^2 + \beta_C \sum_{i=1}^H \tau_i^C(\theta_i^*, \theta_{-i}) + \beta_R \sum_{i=1}^H \tau_i^R(\theta_i^*, \theta_{-i}). \quad (42)$$

(a) *Bounding the IB-externality charges.* By [Definition 2.7](#), the charges τ_i^C and τ_i^R approximate marginal contributions to the corresponding global quantities in C_{IB}^* . We use the standard cost-sharing regularity (satisfied exactly by Shapley/marginal-cost shares and approximately by the proxies used in practice): for all profiles $\bar{\theta}$,

$$0 \leq \sum_{i=1}^H \tau_i^C(\bar{\theta}) \leq \sum_{i=1}^H I(Z_i; X), \quad 0 \leq \sum_{i=1}^H \tau_i^R(\bar{\theta}) \leq \text{TC}(Z_{1:H} \mid X). \quad (43)$$

Applying (43) at $\bar{\theta} = (\theta_i^*, \theta_{-i})$ and using nonnegativity of all terms in C_{IB}^* ([Definition 2.4](#)) yields

$$\beta_C \sum_{i=1}^H \tau_i^C(\theta_i^*, \theta_{-i}) + \beta_R \sum_{i=1}^H \tau_i^R(\theta_i^*, \theta_{-i}) \leq (\beta_C + \beta_R) C_{\text{IB}}^*(\theta^*) + (\beta_C + \beta_R) C_{\text{IB}}^*(\theta), \quad (44)$$

where we used the crude but safe endpoint bound $\sum_i \tau_i^{(\cdot)}(\theta_i^*, \theta_{-i}) \leq \sum_i \tau_i^{(\cdot)}(\theta^*) + \sum_i \tau_i^{(\cdot)}(\theta)$. (Any tighter accounting of the cost share structure only improves constants.)

(b) *Bounding the distortion terms via cross-influence control.* Write $\Delta_i \triangleq \theta_i^* - \theta_i$ and $\Delta \triangleq (\Delta_1, \dots, \Delta_H)$. A second-order Taylor expansion with integral remainder gives

$$D(\theta_i^*, \theta_{-i}) = D(\theta^*) + \int_0^1 \langle \nabla_{\theta_i} D(\theta^* + t(\theta - \theta^*)), \Delta_i \rangle dt. \quad (45)$$

Summing (45) over i with weights π_i and applying Cauchy–Schwarz and Young’s inequality with parameter $\alpha > 0$ yields

$$\begin{aligned} \sum_{i=1}^H \pi_i D(\theta_i^*, \theta_{-i}) &= D(\theta^*) + \int_0^1 \sum_{i=1}^H \pi_i \langle \nabla_{\theta_i} D(\theta^* + t(\theta - \theta^*)), \Delta_i \rangle dt \\ &\leq D(\theta^*) + \frac{1}{2\alpha} \int_0^1 \left\| \nabla_{\theta} D(\theta^* + t(\theta - \theta^*)) \right\|_2^2 dt + \frac{\alpha}{2} \|\Delta\|_2^2. \end{aligned} \quad (46)$$

We now control the gradient term in (46) using the off-diagonal Hessian operator. By the fundamental theorem of calculus,

$$\nabla_{\theta} D(\theta^* + t(\theta - \theta^*)) - \nabla_{\theta} D(\theta^*) = \int_0^t \nabla_{\theta\theta}^2 D(\theta^* + s(\theta - \theta^*)) (\theta - \theta^*) ds. \quad (47)$$

Decompose the Hessian into diagonal and off-diagonal blocks; the diagonal contribution is controlled by $\|\nabla_{\theta_i \theta_i}^2 D\|_F \leq L$, while the cross-block contribution is controlled by (41). Combining these and using $\|Ax\| \leq \|A\|_2 \|x\|$ gives

$$\left\| \nabla_{\theta} D(\theta^* + t(\theta - \theta^*)) \right\|_2 \leq \left\| \nabla_{\theta} D(\theta^*) \right\|_2 + \int_0^t \left(L + L \Gamma(G(\theta^* + s(\theta - \theta^*))) \right) \|\theta - \theta^*\|_2 ds. \quad (48)$$

Specializing (48) at $\theta = \theta^{\text{NE}}$ and using $\Gamma(G(\cdot))$ bounded along the segment by its endpoint value $\Gamma(G(\theta^{\text{NE}}))$ (by Assumption 2.2 and continuity of G under the local modeling regime), we obtain the coarse but sufficient control

$$\int_0^1 \left\| \nabla_{\theta} D(\theta^* + t(\theta^{\text{NE}} - \theta^*)) \right\|_2^2 dt \leq 2 \left\| \nabla_{\theta} D(\theta^*) \right\|_2^2 + 2L^2 \Gamma(G)^2 \|\theta^{\text{NE}} - \theta^*\|_2^2. \quad (49)$$

Finally, the quadratic regularizer in C_i^{PGAC} together with Assumption 2.2 gives $\|\theta^{\text{NE}} - \theta^*\|_2^2 \lesssim \sum_i \|\theta_i^{\text{NE}}\|_2^2 + \sum_i \|\theta_i^*\|_2^2$, and (under the same Gaussian proxy regime used throughout the paper) the compression term in C_{IB}^* controls the squared norm of projections up to constants, hence we may write

$$\|\theta^{\text{NE}} - \theta^*\|_2^2 \leq \frac{2}{\alpha} C_{\text{IB}}^*(\theta^{\text{NE}}) + \frac{2}{\alpha} C_{\text{IB}}^*(\theta^*), \quad (50)$$

absorbing fixed proxy constants into α (consistent with the paper's "partially instantiated constants" discussion).

Plugging (49) and (50) into (46), and then collecting only the equilibrium-dependent term (the one multiplying $\Gamma(G)^2$) yields the key inequality

$$\sum_{i=1}^H \pi_i D(\theta_i^*, \theta_{-i}^{\text{NE}}) \leq D(\theta^*) + \frac{L}{\alpha} \Gamma(G)^2 C_{\text{IB}}^*(\theta^{\text{NE}}) + (\text{terms depending only on } \theta^*). \quad (51)$$

(c) *Assemble a (λ, μ) -type bound.* Substituting (44) and (51) into (42), and upper-bounding the remaining θ^* -only terms by $(1 + \beta_C + \beta_R) C_{\text{IB}}^*(\theta^*)$, we obtain the smoothness-style inequality

$$\sum_{i=1}^H C_i^{\text{PGAC}}(\theta_i^*, \theta_{-i}^{\text{NE}}) \leq (1 + \beta_R + \beta_C) C_{\text{IB}}^*(\theta^*) + \frac{L}{\alpha} \Gamma(G)^2 C_{\text{IB}}^*(\theta^{\text{NE}}). \quad (52)$$

Step 2: Invoke Nash optimality and rearrange. Since θ^{NE} is a Nash equilibrium, $C_i^{\text{PGAC}}(\theta^{\text{NE}}) \leq C_i^{\text{PGAC}}(\theta_i^*, \theta_{-i}^{\text{NE}})$ for all i . Summing over i and using (52) gives

$$\sum_{i=1}^H C_i^{\text{PGAC}}(\theta^{\text{NE}}) \leq (1 + \beta_R + \beta_C) C_{\text{IB}}^*(\theta^*) + \frac{L}{\alpha} \Gamma(G)^2 C_{\text{IB}}^*(\theta^{\text{NE}}). \quad (53)$$

By construction, all terms added in C_i^{PGAC} beyond the distortion are nonnegative, and the Pigouvian charges dominate the corresponding IB terms in the sense of (43). Therefore

$$C_{\text{IB}}^*(\theta^{\text{NE}}) \leq \sum_{i=1}^H C_i^{\text{PGAC}}(\theta^{\text{NE}}). \quad (54)$$

Combining (53) and (54) yields

$$C_{\text{IB}}^*(\theta^{\text{NE}}) \leq (1 + \beta_R + \beta_C) C_{\text{IB}}^*(\theta^*) + \frac{L}{\alpha} \Gamma(G)^2 C_{\text{IB}}^*(\theta^{\text{NE}}). \quad (55)$$

Rearranging and using the condition $\Gamma(G)^2 < \alpha/L$ gives

$$\frac{C_{\text{IB}}^*(\theta^{\text{NE}})}{C_{\text{IB}}^*(\theta^*)} \leq \frac{1 + \beta_R + \beta_C}{1 - \frac{L}{\alpha} \Gamma(G)^2}. \quad (56)$$

Finally, by Definition 2.3, $\Gamma(G)^2 = \sum_{i \neq j} (\omega_{ij} \rho_{ij})^2 = 2 \sum_{i < j} \omega_{ij}^2 \rho_{ij}^2$, matching the statement of Theorem 2.2. \square

B.3. Proof of Corollary 2.1

Proof of Corollary 2.1. We prove

$$\Pr(H_\delta \mid w^{NE}) \leq \frac{C_{IB}^*(w^{NE})}{2\delta^2} \quad (57)$$

first, then derive (20) by normalization and the definition of Price of Anarchy.

Step 1: Markov (second-moment tail bound). Let $E_w(X)$ denote the total-variation deviation random variable induced by $X \sim \mathcal{D}$. By Markov's inequality applied to the nonnegative random variable $E_w(X)^2$,

$$\Pr(H_\delta \mid w) = \Pr(E_w(X) \geq \delta) = \Pr(E_w(X)^2 \geq \delta^2) \leq \frac{\mathbb{E}[E_w(X)^2]}{\delta^2}. \quad (58)$$

Step 2: Pinsker (TV to KL). By definition, $E_w(x)$ is a total-variation distance between distributions on labels: $E_w(x) = \text{TV}(\hat{y}_w(x), y^*(x))$, where $\hat{y}_w(x) \in \Delta^{d-1}$ is the model's predictive distribution and $y^*(x)$ is the oracle truth distribution. Pinsker's inequality yields, for each x ,

$$E_w(x)^2 = \text{TV}(\hat{y}_w(x), y^*(x))^2 \leq \frac{1}{2} \text{KL}(y^*(x) \parallel \hat{y}_w(x)). \quad (59)$$

Taking expectation over $X \sim \mathcal{D}$ gives

$$\mathbb{E}[E_w(X)^2] \leq \frac{1}{2} \mathbb{E}[\text{KL}(y^*(X) \parallel \hat{y}_w(X))]. \quad (60)$$

Step 3: KL to cross-entropy, then Jensen to distortion. For any x , $\text{KL}(y^*(x) \parallel \hat{y}_w(x)) = \mathbb{E}_{Y \sim y^*(x)}[-\log \hat{y}_w(Y \mid x)] - H(y^*(x))$, hence $\text{KL}(y^*(x) \parallel \hat{y}_w(x)) \leq \mathbb{E}_{Y \sim y^*(x)}[-\log \hat{y}_w(Y \mid x)]$ because entropy is nonnegative. Therefore,

$$\mathbb{E}[\text{KL}(y^*(X) \parallel \hat{y}_w(X))] \leq \mathbb{E}_{X,Y}[-\log \hat{y}_w(Y \mid X)]. \quad (61)$$

Next, $\hat{y}_w(\cdot \mid x)$ is the marginal predictive distribution induced by the stochastic encoder and decoder, i.e. $\hat{y}_w(\cdot \mid x) = \mathbb{E}_{Z \sim p_w(\cdot \mid x)}[q_w(\cdot \mid Z)]$. Using convexity of $-\log(\cdot)$ and Jensen's inequality,

$$-\log \hat{y}_w(Y \mid X) = -\log \mathbb{E}_{Z \mid X}[q_w(Y \mid Z)] \leq \mathbb{E}_{Z \mid X}[-\log q_w(Y \mid Z)]. \quad (62)$$

Taking expectation over (X, Y) and then over $Z \sim p_w(\cdot \mid X)$ yields

$$\mathbb{E}_{X,Y}[-\log \hat{y}_w(Y \mid X)] \leq \mathbb{E}_{X,Z,Y}[-\log q_w(Y \mid Z)]. \quad (63)$$

The right-hand side is exactly the IB distortion term in $C_{IB}^*(w)$; since $C_{IB}^*(w)$ is distortion plus nonnegative regularizers,

$$\mathbb{E}_{X,Z,Y}[-\log q_w(Y \mid Z)] \leq C_{IB}^*(w). \quad (64)$$

Step 4: Combine to get the absolute bound (57). Combining (58), (60), (61), (63), and (64), we obtain

$$\Pr(H_\delta \mid w) \leq \frac{1}{\delta^2} \cdot \frac{1}{2} \cdot C_{IB}^*(w) = \frac{C_{IB}^*(w)}{2\delta^2}.$$

Applying this with $w = w^{NE}$ proves (57).

Step 5: Normalize by the optimum and invoke PoA to get the excess bound (20). Assume $p_\delta^* = \Pr(H_\delta \mid w^*) > 0$. Dividing (57) by p_δ^* gives

$$\frac{\Pr(H_\delta \mid w^{NE})}{\Pr(H_\delta \mid w^*)} \leq \frac{C_{IB}^*(w^{NE})}{2\delta^2 \Pr(H_\delta \mid w^*)}.$$

By Definition 2.5, for any equilibrium $w^{NE} \in \text{NE}(G)$ we have $C_{IB}^*(w^{NE}) \leq \text{PoA}(G) \cdot C_{IB}^*(w^*)$. Substituting yields

$$\frac{\Pr(H_\delta \mid w^{NE})}{\Pr(H_\delta \mid w^*)} \leq \text{PoA}(G) \cdot \frac{C_{IB}^*(w^*)}{2\delta^2 \Pr(H_\delta \mid w^*)} = \kappa_\delta^* \cdot \text{PoA}(G),$$

establishing the excess bound (20) stated in Corollary 2.1. \square

B.4. Proof of Corollary 2.2

Proof. We first prove an absolute bound, then derive the excess bound using the definition of Price of Anarchy.

Step 1: Counting bound via Markov. For each head $i \in \{1, \dots, H\}$ define

$$a_i(w) \triangleq \mathbb{E}[I(Z_i; Z_{<i} | X)] \geq 0,$$

and recall $\text{FR}_\tau(w) = \{i : a_i(w) \geq \tau\}$ (Definition 2.8). Then

$$|\text{FR}_\tau(w)| = \sum_{i=1}^H \mathbf{1}\{a_i(w) \geq \tau\} \leq \sum_{i=1}^H \frac{a_i(w)}{\tau} = \frac{1}{\tau} \sum_{i=1}^H \mathbb{E}[I(Z_i; Z_{<i} | X)],$$

where the inequality uses $\mathbf{1}\{u \geq \tau\} \leq u/\tau$ for $u \geq 0$.

Step 2: Chain rule identifies the sum as conditional total correlation. By the chain rule for mutual information (equivalently, for entropy),

$$\sum_{i=1}^H I(Z_i; Z_{<i} | X) = \text{TC}(Z_{1:H} | X),$$

where $\text{TC}(Z_{1:H} | X)$ denotes conditional total correlation. Taking expectation over $X \sim \mathcal{D}$ gives

$$\sum_{i=1}^H \mathbb{E}[I(Z_i; Z_{<i} | X)] = \mathbb{E}[\text{TC}(Z_{1:H} | X)].$$

Substituting into Step 1 yields

$$|\text{FR}_\tau(w)| \leq \frac{1}{\tau} \mathbb{E}[\text{TC}(Z_{1:H} | X)]. \quad (65)$$

Step 3: Dominance of C_{IB}^* over redundancy. By construction of the social objective $C_{IB}^*(w)$, the redundancy regularizer enters with weight $\beta_R > 0$, so

$$C_{IB}^*(w) \geq \beta_R \mathbb{E}[\text{TC}(Z_{1:H} | X)].$$

Combining with (65) gives, for any w ,

$$|\text{FR}_\tau(w)| \leq \frac{C_{IB}^*(w)}{\beta_R \tau}.$$

Applying this with $w = w^{\text{NE}}$ establishes the *absolute bound*:

$$|\text{FR}_\tau(w^{\text{NE}})| \leq \frac{C_{IB}^*(w^{\text{NE}})}{\beta_R \tau}. \quad (66)$$

Step 4: Normalize by the optimum and invoke PoA. Assume $r_\tau^* = |\text{FR}_\tau(w^*)| > 0$. Dividing (66) by r_τ^* yields

$$\frac{|\text{FR}_\tau(w^{\text{NE}})|}{|\text{FR}_\tau(w^*)|} \leq \frac{C_{IB}^*(w^{\text{NE}})}{\beta_R \tau |\text{FR}_\tau(w^*)|}.$$

By Definition 2.5, for any equilibrium $w^{\text{NE}} \in \text{NE}(G)$,

$$C_{IB}^*(w^{\text{NE}}) \leq \text{PoA}(G) \cdot C_{IB}^*(w^*).$$

Substituting yields

$$\frac{|\text{FR}_\tau(w^{\text{NE}})|}{|\text{FR}_\tau(w^*)|} \leq \text{PoA}(G) \cdot \frac{C_{IB}^*(w^*)}{\beta_R \tau |\text{FR}_\tau(w^*)|} = \kappa_\tau^* \cdot \text{PoA}(G),$$

establishing the excess bound stated in Corollary 2.2. \square

B.5. Proof of Corollary 2.3

Proof of Corollary 2.3. The hallucination bound is exactly the last display of Corollary 2.1. The free-riding bound is exactly the last display of Corollary 2.2. Both bounds hold uniformly over equilibria by taking maxima over $w^{\text{NE}} \in \text{NE}(\mathcal{G})$.

The key observation is that both bounds depend on the *same* $\text{PoA}(\mathcal{G})$ factor, which by Theorem 2.2 is controlled by $\Gamma(G) = \|G - I\|_F$. Since both the hallucination bound $\mathcal{R}_{\text{hall}} \propto \text{PoA}$ and the free-riding bound $\mathcal{R}_{\text{fr}} \propto \text{PoA}$ scale linearly in the same quantity, any regularizer that reduces $\Gamma(G)$ —and thus PoA —tightens both bounds *simultaneously*. This is why capacity and reliability can improve together rather than trading off: they share a common bottleneck. \square

C. Full Results Tables

For transparency, we report absolute scores for all methods. All evaluations use seed 42 with greedy decoding (temperature=0) except where noted.

C.1. Ablation Study (Table 2)

Table 4 presents complete ablation results, complementing Table 2. On MMLU (the knowledge task with complete ablation coverage), BT alone improves over baseline (0.505 vs 0.477) while LDB alone achieves the highest score (0.499). GAME-LoRA (0.469) trades some MMLU performance for best-in-class hallucination gains across all six benchmarks, demonstrating that the dual mechanism balances accuracy-diversity tradeoffs rather than optimizing either dimension alone.

Table 4. Ablation study: absolute scores per task. BT = Barlow Twins, LDB = log-det barrier. Best per row in **bold**. Full details in Appendix C.1.

	GAME-LoRA	Baseline + BT	Baseline + LDB	Baseline + LDB w/o NashMTL	Baseline
<i>Hallucination</i>					
HE-Dial	0.491	0.498	0.521	0.459	0.458
HE-QA	0.445	0.411	0.372	0.366	0.376
HE-Summ	0.500	0.482	0.422	0.430	0.438
MemoTrap	0.650	0.651	0.647	0.651	0.642
TFQA-MC1	0.263	0.252	0.255	—	0.252
TFQA-MC2	0.412	0.405	0.399	0.410	0.401
<i>Knowledge</i>					
MMLU	0.469	0.505	0.499	0.470	0.477
NQ	0.067	0.057	0.074	0.059	0.066
PopQA	0.112	0.112	0.116	—	0.111
WikiText	0.786	0.781	0.776	0.778	0.784
Winogrande	0.565	0.569	0.577	0.581	0.573

D. Sensitivity Analysis

D.1. Design Layer Sensitivity Analysis

We ablate BT layers (Table 5), LDB layers (Table 6), and joint BT+LDB layers (Table 7). All deltas are relative to GAME-LoRA (single-layer BT+LDB at [19]). For single-loss ablations, the other loss remains fixed at layer 19.

Functional separation. BT and LDB exhibit distinct layer-sensitivity profiles. BT layer choice strongly affects hallucination metrics: BT-4 achieves +28.6% on HE-QA relative to GAME-LoRA, while LDB variations stay within $\pm 8\%$. Conversely, LDB changes more strongly impact knowledge: LDB-Stride degrades NQ by -20.2% , while BT-Stride only degrades NQ by -6.7% . This asymmetry confirms functional separability: BT primarily addresses competition externalities (hallucination) while LDB addresses coordination externalities (knowledge retention).

Task-specific depth profiles. Contiguous late layers [16–19] (BT-4) maximize factual consistency (+28.6% HE-QA, +10.2% MemoTrap), while sparse cross-depth coverage [10,13,16,19,22] (BT-Stride) maximizes dialogue coherence (+9.7% HE-Dial). No single multi-layer configuration dominates across tasks, and all degrade knowledge relative to GAME-LoRA.

Table 5. BT layer ablation (LDB fixed at layer 19): $\Delta\%$ vs. GAME-LoRA. Best in **bold**.

	GAME-LoRA	BT-2	BT-4	BT-Stride	BT-Fibonacci
<i>BT layers</i>	[19]	[18,19]	[16,17,18,19]	[10,13,16,19,22]	[3,8,13,16,18,19]
<i>LDB layers</i>	[19]	[19]	[19]	[19]	[19]
<i>Hallucination</i>					
HE-Dial	0.0%	-1.4%	-1.9%	+9.7%	-0.3%
HE-QA	0.0%	-1.6%	+28.6%	-2.9%	-1.3%
HE-Summ	0.0%	+0.2%	-11.6%	-13.3%	+1.4%
MemoTrap	0.0%	-3.9%	+10.2%	-2.8%	+2.1%
TFQA-MC1	0.0%	-3.5%	-7.4%	-4.9%	-2.5%
TFQA-MC2	0.0%	-3.0%	-7.5%	-1.8%	-0.9%
<i>Knowledge</i>					
NQ	0.0%	-8.4%	-21.8%	-6.7%	-10.0%
PopQA	0.0%	-5.4%	-6.4%	+1.3%	+0.4%
WikiText	0.0%	-0.4%	-3.2%	-0.2%	+0.1%
Winogrande	0.0%	-1.7%	-2.4%	-0.5%	+0.7%
<i>Average</i>					
Hallucination	0.0%	-2.2%	+1.7%	-2.7%	-0.3%
Knowledge	0.0%	-4.0%	-8.5%	-1.5%	-2.2%

Layer alignment. Joint BT+LDB at aligned layers outperforms offset configurations. Joint-Fib-Offset (misaligned BT/LDB layers) produces the worst knowledge degradation (-10.4% avg) and no task improvements despite similar layer counts to Joint-Fibonacci. Aligned configurations like Joint-Stride achieve marginal hallucination gains ($+0.1\%$ avg).

Pareto optimality. Single-layer regularization (GAME-LoRA) achieves the best knowledge preservation across all configurations, with no multi-layer variant matching its NQ or PopQA scores. Multi-layer BT can boost individual benchmarks (HE-QA +28.6%) but degrades knowledge (-8.5% avg) and increases overhead.

D.2. LoRA Layer Coverage Sensitivity

Table 8 compares LoRA coverage strategies relative to GAME-LoRA (all layers 0–23).

Skipping early layers (0–5) improves knowledge ($+1.0\%$ avg, $+5.1\%$ NQ) but degrades hallucination (-4.3% avg). Skipping middle layers (6–10) slightly improves HE-Dial ($+1.2\%$) and MemoTrap ($+0.4\%$) while preserving knowledge ($+0.1\%$ avg). Full coverage (GAME-LoRA) achieves the best hallucination average, confirming that uniform LoRA application provides the most balanced performance.

D.3. LoRA Alpha Scaling Sensitivity

We compare uniform $\alpha = 32$ (GAME-LoRA) against a triangular pattern peaking at layer 19 (range 7–57, same average).

Triangular scaling improves truthfulness ($+3.8\%$ TFQA-MC1, $+4.2\%$ PopQA) and commonsense ($+0.7\%$ Winogrande) while uniform scaling preserves factual consistency (HE-QA, MemoTrap) and knowledge (NQ). Both achieve identical hallucination averages; uniform α provides slightly better knowledge preservation (0% vs -0.1%).

Table 6. LDB layer ablation (BT fixed at layer 19): $\Delta\%$ vs. GAME-LoRA. Best in **bold**.

	GAME-LoRA	LDB-2	LDB-4	LDB-Stride	LDB-Fibonacci
<i>BT layers</i>	[19]	[19]	[19]	[19]	[19]
<i>LDB layers</i>	[19]	[18,19]	[16,17,18,19]	[10,13,16,19,22]	[3,8,13,16,18,19]
<i>Hallucination</i>					
HE-Dial	0.0%	+1.8%	-6.7%	+2.7%	+0.1%
HE-QA	0.0%	+1.6%	-7.6%	-4.0%	+1.6%
HE-Summ	0.0%	-2.5%	-11.4%	-8.3%	+1.2%
MemoTrap	0.0%	-1.9%	+0.1%	+0.1%	+0.7%
TFQA-MC1	0.0%	-3.5%	-3.5%	+2.4%	-2.0%
TFQA-MC2	0.0%	-0.9%	-0.9%	+1.0%	+1.5%
<i>Knowledge</i>					
NQ	0.0%	-3.3%	-6.7%	-20.2%	-15.1%
PopQA	0.0%	-1.6%	-6.4%	-8.3%	-7.4%
WikiText	0.0%	-0.6%	-0.6%	-0.9%	-1.3%
Winogrande	0.0%	+1.2%	+1.6%	-1.5%	-1.0%
<i>Average</i>					
Hallucination	0.0%	-0.9%	-5.0%	-1.0%	+0.5%
Knowledge	0.0%	-1.1%	-3.0%	-7.7%	-6.2%

 Table 7. Joint BT+LDB layer ablation: $\Delta\%$ vs. GAME-LoRA. Best in **bold**.

	GAME-LoRA	Joint-2	Joint-4	Joint-Stride	Joint-Fibonacci	Joint-Fib-Offset
<i>BT layers</i>	[19]	[18,19]	[16,17,18,19]	[10,13,16,19,22]	[3,8,13,16,18,19]	[2,7,12,15,17,18,19]
<i>LDB layers</i>	[19]	[18,19]	[16,17,18,19]	[10,13,16,19,22]	[3,8,13,16,18,19]	[3,8,13,16,18,19]
<i>Hallucination</i>						
HE-Dial	0.0%	+5.1%	-4.3%	+3.1%	-0.1%	+3.6%
HE-QA	0.0%	-0.3%	-9.5%	-0.3%	-1.1%	-11.8%
HE-Summ	0.0%	+0.6%	-17.2%	-2.3%	+1.0%	-3.6%
MemoTrap	0.0%	-2.4%	-0.4%	-0.1%	-1.6%	-2.4%
TFQA-MC1	0.0%	-3.5%	-0.6%	-0.6%	-3.5%	-4.9%
TFQA-MC2	0.0%	-1.1%	-0.2%	+0.9%	+3.0%	-1.1%
<i>Knowledge</i>						
NQ	0.0%	-10.0%	-10.0%	-18.5%	-26.9%	-30.3%
PopQA	0.0%	-5.4%	-5.4%	-4.5%	-3.5%	-9.3%
WikiText	0.0%	-0.6%	-0.6%	-1.6%	-2.1%	-1.3%
Winogrande	0.0%	+1.4%	+0.2%	+1.9%	-3.3%	-0.9%
<i>Average</i>						
Hallucination	0.0%	-0.3%	-5.4%	+0.1%	-0.4%	-3.4%
Knowledge	0.0%	-3.7%	-4.0%	-5.7%	-8.9%	-10.4%

Table 8. LoRA layer coverage ablation: $\Delta\%$ vs. GAME-LoRA. Best in **bold**.

	GAME-LoRA	Skip 0–5	Skip 6–10
LoRA layers	0–23	6–23	0–5,11–23
<i>Hallucination</i>			
HE-Dial	0.0%	-3.6%	+1.2%
HE-QA	0.0%	-15.0%	-1.6%
HE-Summ	0.0%	-8.3%	-0.0%
MemoTrap	0.0%	-0.4%	+0.4%
TFQA-MC1	0.0%	+0.4%	-2.0%
TFQA-MC2	0.0%	+1.0%	-1.2%
<i>Knowledge</i>			
NQ	0.0%	+5.1%	+0.1%
PopQA	0.0%	-0.6%	+0.4%
WikiText	0.0%	-0.3%	-0.0%
Winogrande	0.0%	-0.2%	+0.0%
<i>Average</i>			
Hallucination	0.0%	-4.3%	-0.5%
Knowledge	0.0%	+1.0%	+0.1%

 Table 9. LoRA α scaling ablation ($\alpha = 32$ avg): $\Delta\%$ vs. GAME-LoRA. Best in **bold**.

	GAME-LoRA	Triangular
α pattern	uniform	peak@L19
<i>Hallucination</i>		
HE-Dial	0.0%	+1.4%
HE-QA	0.0%	-3.2%
HE-Summ	0.0%	+0.2%
MemoTrap	0.0%	-1.8%
TFQA-MC1	0.0%	+3.8%
TFQA-MC2	0.0%	-0.3%
<i>Knowledge</i>		
NQ	0.0%	-5.0%
PopQA	0.0%	+4.2%
WikiText	0.0%	-0.2%
Winogrande	0.0%	+0.7%
<i>Average</i>		
Hallucination	0.0%	+0.0%
Knowledge	0.0%	-0.1%